

New planetary and EB candidates from Campaigns 1-6 of the K2 mission

S. C. C. Barros^{1,2}, O. Demangeon², and M. Deleuil²

¹ Instituto de Astrofísica e Ciências do Espaço, Universidade do Porto, CAUP, Rua das Estrelas, PT4150-762 Porto, Portugal
e-mail: susana.barros@astro.up.pt

² Aix Marseille Université, CNRS, LAM (Laboratoire d'Astrophysique de Marseille) UMR 7326, 13388, Marseille, France

Received ??, ??; accepted ??

ABSTRACT

Context. With only two functional reaction wheels, *Kepler* cannot maintain stable pointing at its original target field and entered a new mode of observation called K2.

Aims. We describe a new pipeline to reduce K2 Pixel Files into light curves that are later searched for transit like features.

Methods. Our method is based on many years of experience in planet hunting for the CoRoT mission. Due to the unstable pointing, K2 light curves present systematics that are correlated with the target position in the CCD. Therefore, our pipeline also includes a decorrelation of this systematic noise. Our pipeline is optimised for bright stars for which spectroscopic follow-up is possible. We achieve a maximum precision on 6 hours of 6 ppm. The decorrelated light curves are searched for transits with an adapted version of the CoRoT alarm pipeline.

Results. We present 172 planetary candidates and 327 eclipsing binary candidates from campaigns 1, 2, 3, 4, 5 and 6 of K2. Both the planetary candidates and eclipsing binary candidates lists are made public to promote follow-up studies. The light curves will also be available to the community.

Key words. planetary systems:detection – stars:K2 –techniques: photometric

1. Introduction

Since the launch of *Kepler* in 2009 (Borucki et al. 2010), the number of confirmed exoplanet has grown exponentially, reaching 2933 known transiting exoplanets today and a few thousand unconfirmed candidates. The great diversity of discovered planetary systems is bringing a number of fundamental clues about the processes of planet formation and evolution. Moreover, *Kepler* has also revealed exoplanets around a diversity of hosts from M-dwarfs (Dressing & Charbonneau 2015) to giant stars (Quinn et al. 2015) and binaries (Doyle et al. 2011).

The exceptional accuracy of the *Kepler* light curves reaching 15 parts per million (ppm) in 6 hours was in part due to its highly stabilised pointing. The failure of two out of four of the reaction wheels of the *Kepler* satellite put an end to prime *Kepler* mission since the pointing stability could not be maintained at the original target field. Fortunately, clever engineering allowed to give a second life to the *Kepler* satellite through a mission named K2 (Howell et al. 2014). K2 is balanced against solar radiation pressure in an unstable equilibrium and it needs to fire thrusters every 6 hours to maintain the pointing.

K2 observes 4 fields a year close to the Ecliptic with a typical duration of 80 days. This important diminution of the time coverage imposed by the new pointing capabilities of the satellite is compensated by the possibility offered to the community to observe different regions of the Milky Way and thus different stellar populations. For example, K2 observes many more M dwarfs than its predecessor (Crossfield et al. 2015; Petigura et al. 2015), but also supernovae, clusters and a full campaign (#9) will be dedicated to microlensing. Furthermore, the targets

observed by K2 are globally brighter facilitating the confirmation and characterisation of the detected planetary systems.

Initially K2 only delivered Pixels files and not light curves. However, since campaign 3, the K2 mission has produced light curves using its PDC pipeline. The initial lack of light curves triggered the development of many K2 pipelines by many groups. The challenge was to correct for the systematics introduced by the degraded pointing stability coupled with a miscalibrated pixel response. To correct these systematics in the K2 data, several methods have been developed all presenting two main steps: a photometric extraction with a variety of aperture shapes and positions and a "correction of systematics". Vanderburg & Johnson (2014) and later on Armstrong et al. (2015) used normal aperture photometry and corrected the systematics decorrelating the flux and the position variations of the target on the CCD. However, while Vanderburg & Johnson (2014) used the fact that the main motion of the line of sight was along 1 direction (the roll direction) which reduced the decorrelation to 1D, Armstrong et al. (2015) opted for a 2D decorrelation. Aigrain et al. (2015) also used aperture photometry but coupled with gaussian processes to model the systematics at the same time as the stellar intrinsic variability. Huang et al. (2015) used the astrometric solution for the position of the targets to extract the light curves and 3 algorithms for the decorrelation of the position related systematics: external parameter decorrelation, trend filtering algorithm (TFA) (Kovács et al. 2005) and semi-periodic stellar oscillations via cosine-filtering. Foreman-Mackey et al. (2015) and Angus et al. (2016) do not decorrelate the systematics but fit the systematics together with their signal of interest respectively transits and periodic signals. They modelled the systematics by identifying common trends in the light curves similarly to the

TFA method. Until now the only pipeline using optimised aperture is the one by Lund et al. (2015). The optimised aperture is calculated with a data clustering algorithm called Density-based spatial clustering of applications with noise (DBSCAN) and their reduction is optimised for asteroseismology studies.

Several groups also performed planet search in the K2 data but only a couple have published lists of planetary candidates: (Foreman-Mackey et al. 2015; Vanderburg et al. 2016) for campaign 0 to campaign 3.

In this paper we present our K2 custom built pipeline and give planetary and binary candidates for stars brighter than $K_p \text{ mag} = 14.7$ from campaigns 1 to 6. In the section 2, we describe the pipeline we developed to extract the K2 light curves and to correct the systematics. In section 3, we discuss the performances of our pipeline. In section 4, we present our method to search for transits in the light curves, our vetting procedure and the results of our eclipse signals hunt for bright stars in the first six campaigns. We finish with a summary of our results in section 5.

2. Data reduction of K2 Pixel files: production of de-correlated light curves

2.1. Photometric extraction

To develop our K2 pipeline, we use several routines from the CoRoT imagerie pipeline (Barros et al. 2014) which is part of the CoRoT legacy. Our main objective being the detection of planetary candidates around bright stars for which follow-up radial velocity observations are possible, we optimised our pipeline for stars whose $K_p \text{ mag} < 15$. Because other targets would require a specific data reduction sequence, we decided to reduce only "Guest Observer Targets" in long cadence and discard superstars.

We download the calibrated pixel data (Pixel Files) from the Mikulski Archive for Space Telescopes (MAST)¹. Then, for each campaign the *Kepler*/K2 science centre provides data release notes which are very useful to identify specific features and events that might affect the photometry. Thus, prior to any reduction step, we take into account the information given in the release notes. We check the start and end cadences and discard custom postage stamps. We also check times of passage of solar system planets in the field of view that can give rise to features in the light curves. Finally, we check for changes in the calibrated pixels pipeline, for example, from campaign 3 the sky background is already subtracted from the postage stamps.

The first step of the pipeline is to extract the header information necessary for our calculations: target magnitude, gain, readout noise, background level and target position. We convert the flux of each pixel to electrons. For simplicity, we consider only images whose QUALITY keyword is equal to zero, except for campaign 2 where 30% of the cadences are accidentally flagged as detector anomalies (flag 16384). While convenient, this strategy has the major drawback of discarding a non-negligible amount of useful data points. Starting in campaign 3, some flags are related to the data reduction process and do not necessarily indicate that the data is unsuitable for high precision photometry. For example, the flag 8192 indicates the possible detection of a cosmic ray hit in the postage stamp (image). As this cosmic ray hit doesn't necessarily affect the PSF of the target stars, the image could be perfectly valid. Therefore we advise

the reader who would like to analyse K2 Pixel files to carefully select which cadences to discard. The details of the flags of the K2 pipeline can be obtained in page 19 of the *Kepler* manual²

The initial lack of official aperture masks³ for the K2 mission required the definition of the target masks which is our second step. Most other K2 pipelines chose circular apertures with several sizes. However, in general the PSF of *Kepler* is neither circular nor symmetric and hence we opt to derive an optimal aperture for each target. This was also done by Lund et al. (2015) that used DBSCAN routine (Ester et al. 1996). In our case, the optimal aperture is calculated with a routine from the CoRoT imagerie pipeline (see Adda (2000) or (Bryson et al. 2010)). The routine requires a mean image, the gain and the mean background level. To avoid contamination by background stars, for non saturated stars ($K_p \text{ mag} > 10$), we considered a 9 by 9 pixel subset of the original image centred in the position of the target taken from the header. Subsequently, pixels from this mean sub-image are ranked by decreasing flux. Then they are added starting by the highest flux pixel until the total signal-to-noise ratio starts to decrease. Finally, in order to obtain a connected aperture, the routine excludes pixels that are isolated. Therefore, contaminating stars that are separated from the main target are not included in the mask but targets whose PSF merge with the main target are included in the mask to decrease the noise. This results in apertures that are in general not circular, contrary to most of the other published K2 pipelines, and nicely follow the PSF shape. However, we found that for saturated stars the mean image resulted in a PSF that was too short along the main saturation column. This is because the extent of the saturation leakage strongly depend on the flux. Therefore, for stars brighter than 10 mag we apply the optimum aperture routine to the mean of the 10 brightest images which are the ones with the larger PSF. The saturated stars have very large optimal apertures ranging from 100 pixels to 900 pixels. We also found that, for stars brighter than 16 mag, increasing the optimal aperture by 1 pixel all around the aperture improved the final light curve. This results in apertures with 10-50 pixels in the brightness range between 10 and 16 mag. This enlargement of the optimal aperture was not needed for CoRoT but it is probably required here because of the additional pointing jitter. Finally in some cases, mostly for faint stars (16-20 mag), the signal-to-noise always increases by adding new pixels. Therefore, the resulting aperture is the whole imagerie and we consider that the aperture fails. For these cases, we performed some tests, concluded that the best aperture was as small as possible and we use the smallest practical aperture containing 3x3 pixels. We show two extreme examples of our mask in Figure 1.

The third step consists in computing and removing the background flux level for campaigns 0-2. For later campaigns the background flux level was already removed so this step is not performed. We estimate the background level using the 3σ clipped median of all the pixels in the image that are not inside the aperture mask and we remove the background from each image.

The fourth step is the computation of the centroid position. Since the centroid position is very important for the correction of the flux-position systematics, we tested several algorithms to calculate the centroid. We found that the Modified Moment Method by Stone (1989) resulted in a smaller dispersion in the final light curves. Therefore, we choose this method that was also used in the CoRoT imagerie pipeline.

² http://archive.stsci.edu/kepler/manuals/archive_manual.pdf

³ For the campaigns 3 and after, the K2 mission is also producing aperture masks.

¹ http://archive.stsci.edu/kepler/data_search/search.php

¹ <http://keplerscience.arc.nasa.gov/>

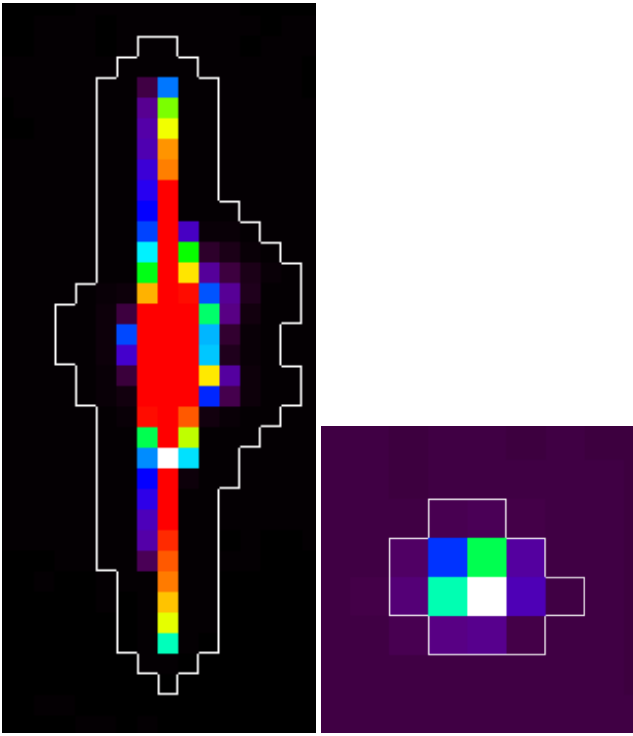


Fig. 1. Example of aperture mask for EPIC 201832337, a 7.8 mag star that shows high saturation (left panel) and EPIC 201465501, a 15 mag star (right panel).

In the final step, for each image, we compute the sum of all the flux inside the optimal aperture. We also compute the corresponding uncertainty which accounts for photon statistics, read-out noise and the noise of the subtracted background. The light curves are normalised to 1 by dividing by the mean flux. At this stage, the light curves are called "raw light curves" (RAWLC). An example of a raw light curve is shown in the left of Figure 2.

2.2. Flux-Position decorrelation

The degraded pointing stability of the K2 mission couples with pixel sensitivity variations to introduce systematics in the raw light curves as it is clear in Figure 2. As mentioned above, several methods to correct the systematics have been applied to the K2 data (Vanderburg & Johnson 2014; Aigrain et al. 2015; Foreman-Mackey et al. 2015; Armstrong et al. 2015; Lund et al. 2015). In our case to correct for this flux dependence with position we used a procedure similar to Vanderburg & Johnson (2014) which is based on methods developed for the Spitzer satellite (Knutson et al. 2008; Ballard et al. 2010; Stevenson et al. 2012). Due to the particular pointing stabilisation mechanism of K2, the satellite slowly rolls around its line of sight and to correct for this, every 6 hours, the thrusters are fired returning the spacecraft close to its initial orientation. Thus, Vanderburg & Johnson (2014) showed that for each roll of the spacecraft, the target crosses a similar path on the CCD. This allows the use of self-flat-fielding methods which calibrate the sensitivity variations with respect to the centroid position of the target by calculating the mean flux at each of a series of centroid position bins. Then the flux can be corrected from those sensitivity changes. The authors showed that they could retrieve a precision within a factor of 2 of the *Kepler* primary mission.

Following Vanderburg & Johnson (2014), we start by estimating and removing stellar activity with a spline filter with

breakpoints every 1.5 days. Then we calculate the main direction of motion using principal component analysis. Finally, the sensitivity dependence with position is computed and the correction is applied to the data. This 1D approximation starts failing after ~ 10 days due to an extra slow drift of the satellite along the direction perpendicular to the main rolling motion. Hence, to maintain the 1D approximation, the light curves are divided in 8 segments. The division is mostly in equal parts but we insure that there are divisions whenever the position behaviour changes. For example in Campaign 1, the satellite pointed towards the Earth in the middle of the campaign to download data. This created a gap in the data and a drastic change of correlation between flux and position before and after the gap. For the other campaigns similar breaks happen although not always for the same reasons. For each segment we performed the decorrelation method described above. After this self-flat-fielding procedure the stellar activity signal, filtered out by the spline filter, is re-added to the light curve to avoid affecting the transit shape. In right panel of Figure 2 we show the light curve of the same target as in left panel, EPIC 201465501, after the flux-position decorrelation with our pipeline.

The precision of the centroid is very important for the performances of the decorrelation. The precision on the centroid is better for bright stars that are not saturated. Hence, for each of the 21 modules of K2 we choose a non saturated bright star and used its centroid position to decorrelate all the stars of the same module. This resulted in final light curves with smaller RMS than if we use individual centroid positions especially for stars fainter than 14 mag.

We also investigated flux-position decorrelation using a 2D self-flat-fielding procedure. We start by removing stellar activity as explained above. Then we compute a 2D map of the variation of sensitivity with position with 40 bins in the main direction of motion and 20 bins in the other direction. The sensitivity dependence with position was corrected by dividing the light curve by the respective interpolation of the 2D flat field map. In agreement with Lund et al. (2015), we find that the previously described 1D procedure corrects better the flux-position correlation than the 2D flat fielding and opt for it for our pipeline. This is because the 2D procedure is very sensitive to the bin size, for too small bin sizes we are over-fitting the data and for too large bin sizes the interpolation is not sufficient to describe correctly the sensitivity variations resulting in a poor correction. Further optimisation of this 2D self-flat-fielding method is possible and Armstrong et al. (2015) showed that it also gives nice results.

Our pipeline produces two data products, the decorrelated light curve described above, thereafter `DECLC`, and a light curve where the stellar activity has been filtered, thereafter `FILLC`, which is used to search for transits and for performance analysis. To obtain the `FILLC`, we filter stellar activity on timescales longer than 0.5 days with a spline filter with break points every 0.5 days. Then we reject points that are 5 sigma higher than the median. Points that are 5 sigma lower than the median are only rejected if the points immediately before and after are not 5 sigma lower than the median to avoid removing transits. This sigma rejection is needed to remove remaining cosmic ray hits and points for which the decorrelation didn't work.

3. Photometric performance

To improve and optimise the performance of the pipeline, we performed several tests on the filtered light curves. For each light curve, we computed four statistical indicators: the robust RMS (i.e. root mean square with 3 sigma clipping), the mean

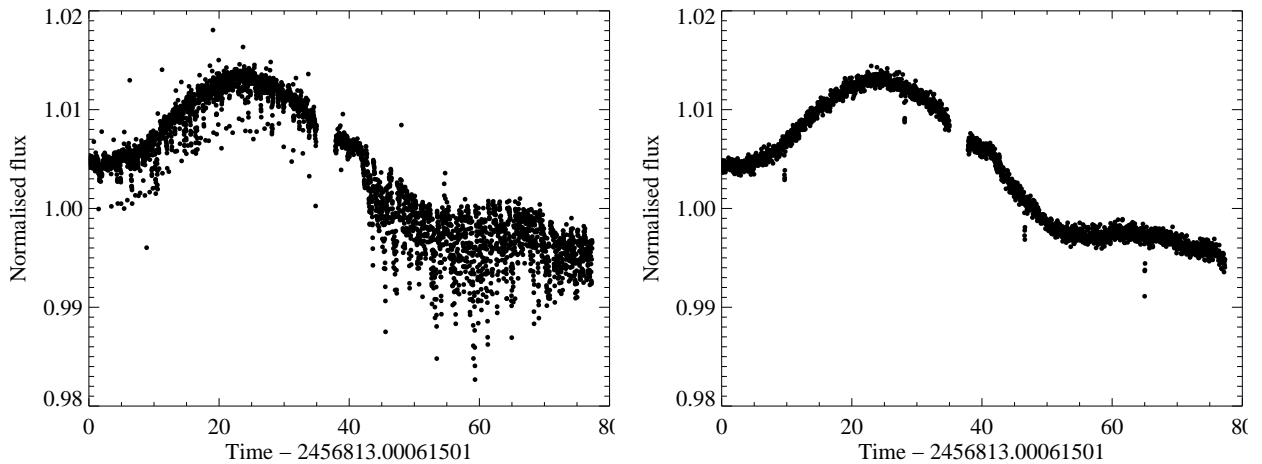


Fig. 2. Left panel: The large systematic noise is clearly visible on the raw light curve of EPIC 201465501, a 14.95 magnitude star in Campaign 1. Right panel. Same light curve after being position-decorrelated. The improvement of the precision is evident, the rms improved from 1358 ppm for the RAWLC to 417 ppm for the DECLC, allowing to clearly see the transits.

point to point variation (P2P) and the quasi Combined Differential Photometric Precision (CDPP) measured on 2.5 and 6 hours timescales (used to approximate the real CDPP provided with *Kepler* data, Christiansen et al. (2012)). This quasi-CDPP was obtained by computing the standard deviation within a running window of 2.5 or 6 hours window divided by the square root of the number of points in each bin (Vanderburg & Johnson 2014). In most cases, the conclusions drawn from all the statistics indicators agree.

We performed in depth testing for campaign 1 and 3, but for concision and clarity, we only show here the results obtained on campaign 3 (C3) for which we reach a lower noise level. However, the performance for both campaigns is qualitatively the same. The lower noise level of campaign 3 onwards is due to the increase in the frequency of pointing corrections.

3.1. Pipeline tests

As mentioned above we tested the centroid computation and the size of the aperture and optimised them in order to obtain a lower robust RMS in the final light curve. We also tested if moving the aperture to make it follow the centroid motion, thereafter "jitter correction", would improve and/or be sufficient to correct the flux-position systematics. To do this, we used a routine developed for the CoRoT imagerie pipeline. This routine oversamples the images, re-centres them to superimpose the centroids of all the images and finally converts them back to the original sampling. The result is similar to aperture shifting at sub-pixel level. If the flux correlation with position was due to aperture losses only, this procedure would completely correct the effects of the pointing jitter. It would be more efficient than just increasing the size of the aperture since it prevents from increasing the background noise.

In Figure 3, we show the robust RMS of each RAWLC not decorrelated but where the stellar activity has been filtered out, both with and without jitter correction. We find that correcting the jitter improves the photometry for stars fainter than 11 mag but degrades it for brighter stars. 11 mag being very close to the 11.3 mag of *Kepler* saturation level (Gilliland et al. 2010), we conclude that for saturated stars correcting the jitter degrades the photometry. Noteworthy, even for the faint stars, the jitter correction is not enough to completely correct the flux-position

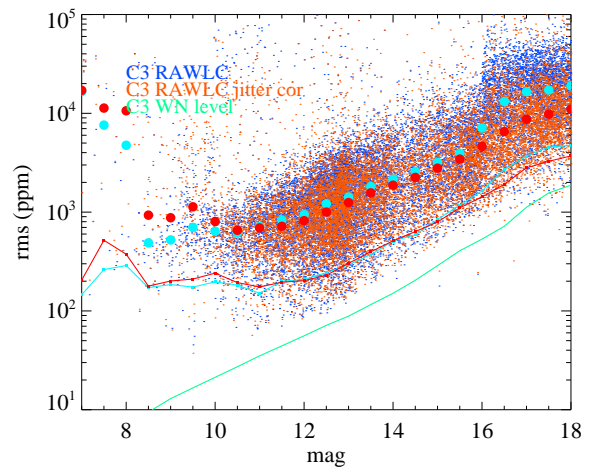


Fig. 3. Robust RMS of the raw light curves, with the stellar activity filtered, before (black) and after (red) jitter correction in C3. We show the median of the RMS in bins of 0.5 mag as large circles and the lower RMS envelope computed with the 0.05 percentile with the respective colour code. We also show the median of the light curves estimated uncertainties assuming only white noise (green line) for comparison with other figures.

dependence (as one can see comparing Figure 3 with the top-left panel of Figure 4). Therefore, we conclude that the main reason for the degradation of the precision of the light curves from K2 relative to *Kepler* is intra/extra pixel sensitivity variations and not aperture losses. Hence, the systematics need to be corrected with the decorrelation techniques presented above.

We also tested if the jitter correction would improve the RMS of the decorrelated light curves. We found that the jitter correction actually increases the RMS of the final light curves. This is probably because the PSF is very under-sampled and the jitter correction actually introduces noise. In contrast, the CoRoT PSF was much better sampled and the same routine worked very well for CoRoT imagerie data.

3.2. Pipeline performance

To exemplify the final performance of the pipeline described in section 2, we show the comparison of the four statistical indi-

Table 1. Minimum values of the RMS, p2p, CDPP2.5 and CDPP6 achieved in each campaign.

Campaign	RMS (ppm)	p2p (ppm)	CDPP2.5 (ppm)	CDPP6 (ppm)
C1	43	56	17	13
C2	45	48	15	16
C3	29	39	12	9
C4	22	24	7	6
C5	19	22	7	6
C6	21	23	7	6

cators for the stellar activity filtered RAWLC and the FILLC light curves of C3 in Figure 4. We show the results for each individual light curve together with the median in each 0.5 mag bin (large filled circles) and the lower envelope computed with the 0.05 percentile (red and blue lines) for clarity. The decorrelation increases significantly the photometric precision according to all indicators and also decreases the spread of values in each magnitude bin. The improvement of the decorrelation is higher for the RMS (median decrease of 2022 ppm) and CDPP6 (median decrease of 560 ppm) indicators which are particularly sensitive to long timescales where the 6 hours systematic noise due to pointing is more evident. We conclude that the final photometric precision approaches the white noise level and it is similar to the precision obtained in the nominal *Kepler* mission. Noteworthy, as in *Kepler* we found a red noise, residual of stellar activity (Bastien et al. 2016), in the light curves that prevents us from reaching the white noise level.

In Table 1 we show the minimum values of the RMS, p2p, CDPP2.5 and CDPP6 for each campaign. After campaign 3, we reach a precision similar to the original *Kepler* mission. For the earlier campaigns we find slightly higher noise levels. This confirms the improvement of photometric precision during and after campaign 3 caused by the smaller motion of the satellite during exposures. Hence we conclude that our pipeline is capable of correcting the position dependence and achieves similar performance to other published pipelines.

The light curves computed by our pipeline have been used in several published papers. The light curves of K2-3 (Almenara et al. 2015) and K2-19 (Barros et al. 2015) were used to better characterise these two multi-planetary systems. For the 11.6 magnitude star, K2-3, we achieved an robust RMS of the FILLC of 115ppm. For K2-19 which is a 12.8 magnitude star we achieved a RMS of 175ppm. Our light curves were also used in the discovery papers of EPIC-211089792b (Santerne et al. 2016), EPIC-210957318b and EPIC-212110888b (Lillo-Box et al. 2016) and EPIC-212521166b (Osborn et al. in prep.). The host stars have magnitudes of 12.9, 13.2, 11.4, 11.6 and the corresponding light curves (FILLC) produced by our pipeline have a robust RMS of 195ppm, 368 ppm, 86 ppm and 134 ppm respectively.

4. Transit search and candidates vetting

For the transit search, we use the filtered light curves (FILLC) and an adapted version of the CoRoT alarm pipeline (Bonomo et al. 2012). We only performed this search on targets brighter than $K_p \text{ mag} = 14.7$ for which follow-up radial velocity is possible. For this bright targets we can obtain a good precision on both planetary mass and radius and hence probe the planetary composition.

The CoRoT alarm pipeline starts by filtering out any undesired signals from the light curves. For this purpose, the first step

consists in identifying outliers caused by non corrected cosmic ray hits thanks to a 5-sigma clipping. Then the remaining low-frequency signals (residual of the stellar activity and pointing jitter noise) are corrected with a high-pass filter realised by removing a 0.5 days sliding median. High-frequency variations are removed with a low-pass Savitzky-Golay filter (Press et al. 1992) with a time scale of ~ 1 h to preserve transit ingress and egress. Finally discontinuities ("jumps"), which are produced by hot pixels or sudden pointing jitter (see for e.g. Srour et al. (2003) or Auvergne et al. (2009)) and filtered by the previous steps, can produce a lot of instrumental false positives when looking for transit signals. Therefore, they are detected using a moving window of eight data points and computing the standard deviation inside this moving window. If the standard deviation differs of more than 4 sigma from the mean standard deviation, a discontinuity is detected. In order to avoid transient effects associated with the appearance of hot pixels or with the filtering of a pure discontinuity, we remove 0.4 days before and after the time of each discontinuity.

After the filtering steps, the transit hunt is performed with a Box-fitting Least-Square (BLS) algorithm with the directional correction (Tingley 2003) that eliminates from the resulting periodogram box-shaped events with a negative depth. The search is made over periods ranging from 0.4 to 50 days and durations ranging from 0.006 to 0.09 times the period with a number of phase bins $n_{\text{bins}} = 240$ (Kovács et al. 2002). The frequency sampling is optimised according to the criterion given by $\delta\nu = 1/(P_{\text{max}} \cdot n_{\text{bins}})$ where P_{max} is the maximum period searched (Schwarzenberg-Czerny & Beaulieu 2006). Using the periods and epochs found by the BLS, each light curve is phase-folded and the signal detection (SD) efficiency is computed (Kovács et al. 2002). We obtain a few thousand eclipse signal detections per campaign, most of which are instrumental false positives. Hence, the candidates have to be screened and we inspect by eye all the folded light curves up to a SD of 11, which was empirically chosen after scrutinising the results of the first 3 campaigns.

The light curves that have real transit-like events are then divided between planetary candidates and eclipsing binary candidates. First, to avoid misidentification of the correct period, we test the double and half of the detected period. Then we fit independently a trapezoidal model to the phase-folded primary transit, and to the phase-folded odd and even primary transits. We also look for the presence of a secondary transit fitting a trapezoidal model with the same outer and inner durations as the primary transit, but leaving the depth as a free parameter in the vicinity of the 0.5 orbital phase (from 0.4 to 0.6 with a visual inspection outside of this range). Finally we perform a visual search for sinusoidal out-of-transit variations. With all this information, we perform a list of checks which, if any of them is true, allow us to decide that a candidate should be classified as an eclipsing binary:

- Candidates with sinusoidal out-of-transit variations;
- Candidates with a significant difference in the depth of the odd and even transits;
- Candidates with depth higher than 5%;
- Candidates with a significant secondary transit and a period longer than 2 days.

For candidates with a significant secondary transit and a period shorter than 2 days, the decision is taken on a case by case basis, taking into account the depth of this secondary transit and the other criteria above.

The results of this hunt for the campaign 1 to 6 of K2 are provided in Table 3 for the planetary candidates and in Table 5

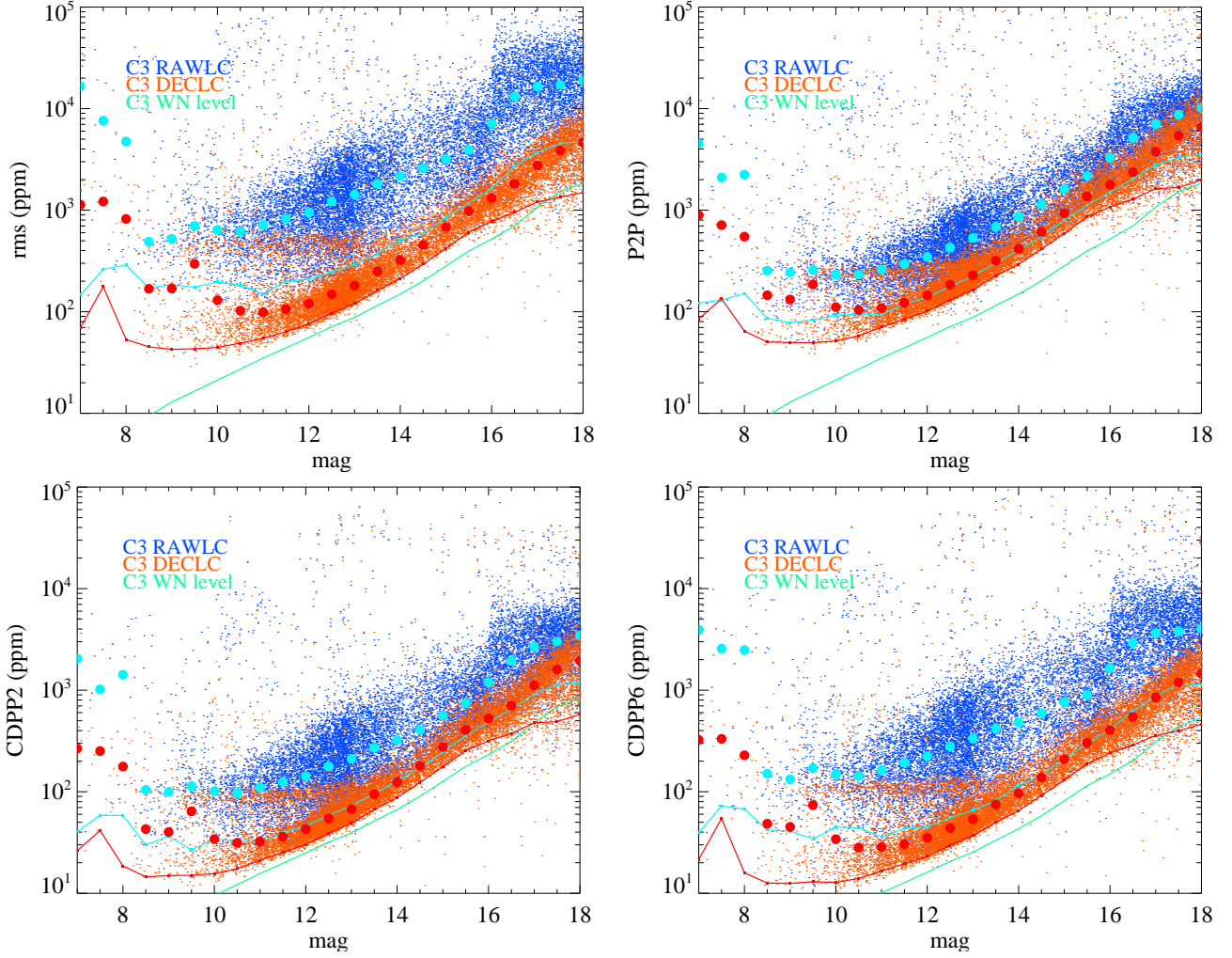


Fig. 4. Robust RMS of light curves, with the stellar activity filtered, before (black) and after (red) the position decorrelation. For each statistic, we show the median value in each 0.5 mag bin as large circles and the lower envelope computed with 0.05 percentile with the respective colour code. We also show the median of the light curves estimated uncertainties assuming only white noise (green line).

Table 2. Number of planetary and eclipsing binary candidates found per campaign.

Campaign	Planetary	EB	Total LC
C1	19	35	8743
C2	20	59	10609
C3	22	38	9261
C4	27	60	10650
C5	58	60	16077
C6	26	75	16841

for the eclipsing binary candidates. In these tables, we present the period, epoch, depth, full duration of the transit/eclipse and ingress/egress duration. We also give a few indicators that the reader can use to choose their favourite targets depending on their science objectives: existence of secondary and V-shaped (grazing) at a 3 sigma detection threshold. We consider that a transit is V-shaped if the time between the 2nd and 3rd contacts is $0 \pm 3 \sigma_{t23}$. In some cases with low signal-to-noise ratio our automatic trapezoidal fit gives excessively high error bars for some parameters, these were substituted by *.

In Table 2, we show a summary of the number of planetary and EB candidates found in each campaign. For campaigns 1 to

3, there are already two published lists of planetary candidates provided by Foreman-Mackey et al. (2015) and Vanderburg et al. (2016), hence some of these candidates were already followed up, confirmed or disconfirmed. For campaign 1, we found 5 new candidates compared to these two lists: EPIC 201534540, 201291843, 201270464, 201705526 and 201626686. We found 9 new planetary candidates for campaign 2: EPIC 203623230, 204658292, 204763194, 203560204, 204346718, 204676499, 205047565, 205050711 and 202688980. Furthermore, we found 4 new planetary candidates for campaign 3: EPIC 206175552, 206311743, 206500801, 206152015. Finally, we present here the first published list of planetary candidates for campaigns 4, 5 and 6.

For the early campaigns, we missed some candidates that were already found by others in stars within our magnitude limit (brighter than 14.7 mag): 29 in C1, 23 in C2 and 36 in C3. The majority of these false negatives were due to the incorrect identification of the period by the BLS due to noise. In few cases the BLS identified an harmonic of the real period. Very few were missed because they had a SD value lower than our limit. Future improvements of our pipeline will attempt to reduce this number of false negatives. All transit surveys and detection efforts suffer from incompleteness. Therefore, it is always beneficial to have

several groups publishing their candidate lists so that together we miss the least amount of real candidates.

In most campaigns we find the double of eclipsing binaries candidates (0.4-0.6 %) than planetary candidates (0.2-0.25 %) except for campaign 5 where the number of candidates in both categories are almost the same (0.36%). In the latest campaigns C5 and C6 the number of light curves within our magnitude cut has increased by 50%. However they also have a higher percentage of faint stars (13.5-14.5 bin) where planets are more difficult to detect. This explains the disproportional increase in the number of candidates for these campaigns.

In Figure 5, we show histograms of the orbital period and depth of planetary and EB candidates that we found. We find a large percentage of candidates with small depths. The lowest is 0.008%, which corresponds to a planetary radius of $0.975 R_{\oplus}$ (if orbiting a solar size star). The shorter baseline combined with higher systematic noise leads to a lower limit on the transit depth than the nominal *Kepler* mission. We also find a large percentage of candidates with short periods. The main reason for this is observational biases, since the transit probability decreases as $P^{-2/3}$. We also require at least two transits to be observed to claim a detection. Therefore, we expect a large incompleteness for periods longer than 40 days. All of this planetary candidates have magnitudes brighter than 14.7 mag and amongst them 128 planetary candidates have magnitudes brighter than 12. These will be excellent targets for measuring accurate mass and radius, probing the planetary composition and for atmospheric studies.

5. Summary

We provide decorrelated light curves for all long cadence targets of K2 from C1 to C6 (discarding superstamps). The particularity of our pipeline relative to previously published ones is the determination of an optimal aperture and the precision of the centroid determination. Our apertures are in general not circular and follow nicely the PSF of the stars. We show that our light curves have precision similar to the light curves from the nominal *Kepler* mission and they will be made public.

Using these light curves we searched for eclipse signals on targets brighter than 14.7 magnitudes. This analysis results in a list of 172 planetary and 327 EB candidates. Among the 172 planetary candidates, 129 are new while this is the first release of eclipsing binary candidates from K2 data. All these products will be made public. Other teams have presented candidates for the K2 data till campaign 3. The different methods lead to common and non common candidates since the pipelines have slightly different performances for specific targets. The comparison between the methods will allow to fine tune the methods themselves but most importantly to build a more robust candidate list.

There are some possible improvements to the pipeline like, for example, application to the short cadence data, and/or a more robust transit search, an automatic candidate validation instead of the current eyeballing that could result in larger number of candidates. However we think that making candidate lists available is urgent in order to optimise the follow-up of candidates and prevent waste of resources.

Acknowledgements. SCCB acknowledges support by grants 98761 by CNES and the Fundação para a Ciência e a Tecnologia (FCT) through the Investigador FCT Contract No. IF/01312/2014 and the grant reference PTDC/FIS-AST/1526/2014 through national funds and by FEDER through COMPETE2020 (ref. POCL-01-0145-FEDER-016886). OD acknowledges support by the CNES grant 124378. We thank the referee for his/her valuable information.

References

- Adda, M. 2000, (Doctoral thesis, Université Paris 6, Paris, France, 166)
- Aigrain, S., Hodgkin, S. T., Irwin, M. J., Lewis, J. R., & Roberts, S. J. 2015, *MNRAS*, 447, 2880
- Almenara, J. M., Astudillo-Defru, N., Bonfils, X., et al. 2015, *A&A*, 581, L7
- Angus, R., Foreman-Mackey, D., & Johnson, J. A. 2016, *ApJ*, 818, 109
- Armstrong, D. J., Kirk, J., Lam, K. W. F., et al. 2015, *A&A*, 579, A19
- Auvergne, M., Bodin, P., Boissard, L., et al. 2009, *A&A*, 506, 411
- Ballard, S., Charbonneau, D., Deming, D., et al. 2010, *PASP*, 122, 1341
- Barros, S. C. C., Almenara, J. M., Deleuil, M., et al. 2014, *A&A*, 569, A74
- Barros, S. C. C., Almenara, J. M., Demangeon, O., et al. 2015, *MNRAS*, 454, 4267
- Bastien, F. A., Stassun, K. G., Basri, G., & Pepper, J. 2016, *ApJ*, 818, 43
- Bonomo, A. S., Chabaud, P. Y., Deleuil, M., et al. 2012, *A&A*, 547, A110
- Borucki, W. J., Koch, D., Basri, G., et al. 2010, *Science*, 327, 977
- Bryson, S. T., Tenenbaum, P., Jenkins, J. M., et al. 2010, *ApJ*, 713, L97
- Christiansen, J. L., Jenkins, J. M., Caldwell, D. A., et al. 2012, *PASP*, 124, 1279
- Crossfield, I. J. M., Petigura, E., Schlieder, J. E., et al. 2015, *ApJ*, 804, 10
- Doyle, L. R., Carter, J. A., Fabrycky, D. C., et al. 2011, *Science*, 333, 1602
- Dressing, C. D. & Charbonneau, D. 2015, *ApJ*, 807, 45
- Ester, M., Krieger, H.-P., Sander, J., & Xu, X. 1996, in (AAAI Press), 226–231
- Foreman-Mackey, D., Montet, B. T., Hogg, D. W., et al. 2015, *ApJ*, 806, 215
- Gilliland, R. L., Jenkins, J. M., Borucki, W. J., et al. 2010, *ApJ*, 713, L160
- Howell, S. B., Sobeck, C., Haas, M., et al. 2014, *PASP*, 126, 398
- Huang, C. X., Penev, K., Hartman, J. D., et al. 2015, *MNRAS*, 454, 4159
- Knutson, H. A., Charbonneau, D., Allen, L. E., Burrows, A., & Megeath, S. T. 2008, *ApJ*, 673, 526
- Kovács, G., Bakos, G., & Noyes, R. W. 2005, *MNRAS*, 356, 557
- Kovács, G., Zucker, S., & Mazeh, T. 2002, *A&A*, 391, 369
- Lillo-Box, J., Demangeon, O., Santerne, A., et al. 2016, *ArXiv e-prints* [arXiv:1601.07635]
- Lund, M. N., Handberg, R., Davies, G. R., Chaplin, W. J., & Jones, C. D. 2015, *ApJ*, 806, 30
- Petigura, E. A., Schlieder, J. E., Crossfield, I. J. M., et al. 2015, *ApJ*, 811, 102
- Press, W. H., Teukolsky, S. A., Vetterling, W. T., & Flannery, B. P. 1992, *Numerical recipes in FORTRAN. The art of scientific computing*
- Quinn, S. N., White, T. R., Latham, D. W., et al. 2015, *ApJ*, 803, 49
- Santerne, A., Hébrard, G., Lillo-Box, J., et al. 2016, *ArXiv e-prints* [arXiv:1601.07680]
- Schwarzenberg-Czerny, A. & Beaulieu, J.-P. 2006, *MNRAS*, 365, 165
- Srouf, J. R., Marshall, C. J., & Marshall, P. W. 2003, *IEEE Transactions on Nuclear Science*, 50, 653
- Stevenson, K. B., Harrington, J., Fortney, J. J., et al. 2012, *ApJ*, 754, 136
- Stone, R. C. 1989, *AJ*, 97, 1227
- Tingley, B. 2003, *A&A*, 408, L5
- Vanderburg, A. & Johnson, J. A. 2014, *PASP*, 126, 948
- Vanderburg, A., Latham, D. W., Buchhave, L. A., et al. 2016, *ApJS*, 222, 14

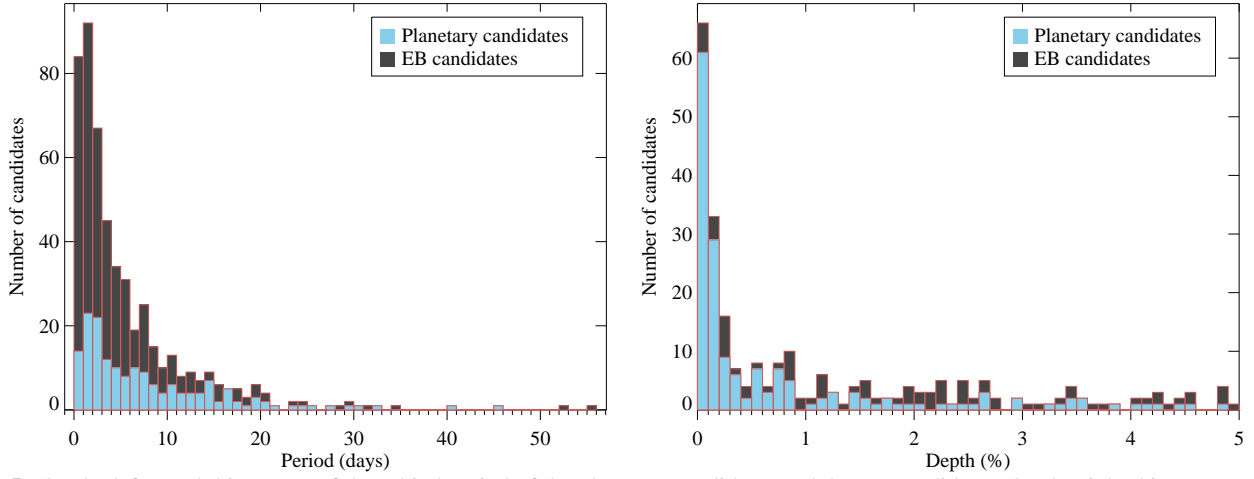


Fig. 5. On the left panel: histogram of the orbital period of the planetary candidates and the EB candidates. On the right: histogram of the depth of the planetary candidates and EBs with depth $< 5\%$.

Table 3. Parameter for the planet candidates

EPIC	mag	RA	DEC	Period	T0	Depth %	T ₁₄ (h)	T ₁₂ (h)	Sec	Gr
Campaign 1										
201208431	14.41	11:38:58.9536	-3:54:20.106	10.00617969	6815.5130268	0.130±0.011	3.036±0.401	0.522±0.344	-	Y
2012070176	12.45	11:20:31.8235	-2:54:09.2952	1.57771549	6818.3269951	1.823±0.121	3.086±0.148	1.280±0.153	-	Y
201270464	9.39	11:20:32.0352	-2:53:53.4084	1.57771549	6818.3276907	0.875±0.012	2.993±0.034	1.203±0.032	-	-
201291843	13.68	11:53:41.0021	-2:34:18.3936	40.70206194	6823.2949209	0.536±0.028	1.621±4.980	0.089±4.838	Y	Y
201324549	12.15	11:24:56.6198	-2:05:06.5904	2.51881781	6820.0759662	0.215±0.007	1.580±0.057	0.790±0.028	-	-
201367065	11.57	11:29:20.3878	-1:27:17.2332	10.05176778	6823.4776686	0.145±0.004	3.052±0.118	0.829±0.096	-	-
201445392	14.38	11:19:10.4796	-0:17:03.75	10.35848367	6813.5958020	0.149±0.014	3.263±0.243	1.134±0.253	-	Y
201505350	12.81	11:39:50.4766	+0:36:12.87	7.91952314	6829.222756	0.667±0.009	3.415±0.078	0.612±0.063	Y	-
201534540	8.20	11:26:36.2808	+1:03:18.8388	2.72273204	6814.4918318	1.494±0.178	3.596±0.256	1.562±0.292	-	Y
201546283	12.43	11:26:03.6396	+1:13:50.6568	6.77093147	6819.6205997	0.267±0.003	3.032±0.046	0.580±0.039	-	-
201549860	13.92	11:20:24.7394	+1:17:09.4416	5.60967748	6817.7182408	0.093±0.009	2.290±0.282	0.723±0.239	-	Y
201577035	12.30	11:28:29.2697	+1:41:26.2896	19.29206200	6819.6007738	0.164±0.009	4.413±0.263	1.594±0.208	-	Y
201596733	14.28	11:22:42.9838	+1:59:35.7936	2.89607106	6815.0048603	0.383±0.072	1.874±0.603	0.501±0.535	-	Y
201626686	11.47	11:17:47.3047	+2:27:21.6216	5.28130579	6817.6339628	0.074±0.005	3.552±0.298	0.837±0.244	Y	Y
201705526	9.94	11:29:32.5939	+3:43:55.5816	18.10220826	6831.4965980	0.780±0.006	4.521±0.028	1.697±0.025	-	-
201713348	11.53	11:17:47.7775	+3:51:59.0148	5.34107237	6818.1463447	0.163±0.000	-0.068±0.000	-0.034±0.000	Y	-
201779067	11.12	11:14:10.2478	+4:59:17.2716	27.27048734	6820.2309771	3.413±0.170	6.748±0.280	2.785±0.254	-	Y
201785059	14.60	11:22:47.4377	+5:05:43.2996	1.39533316	6814.3842864	0.054±0.005	1.180±0.399	0.201±0.355	-	Y
201862715	10.25	11:43:38.0112	+6:33:49.4136	2.65662719	6818.2485688	1.459±0.023	3.025±0.056	0.916±0.046	-	-
201912552	12.47	11:30:14.5104	+7:35:18.2076	32.92801934	6836.1797950	0.354±0.021	3.776±0.256	1.888±0.128	-	-
Campaign 2										
202688980	11.77	16:16:52.9858	-28:43:49.1592	1.45566370	6896.6370171	2.958±0.036	2.512±0.033	1.256±0.017	-	-
202710713	12.24	16:16:16.0565	-28:38:56.8788	3.32592848	6898.7028983	0.091±0.004	4.655±0.232	1.232±0.183	-	-
203294831	11.57	15:59:31.0104	-26:36:15.7212	1.85872487	6897.3878216	4.143±0.112	3.213±0.068	1.291±0.067	-	-
203560204	14.63	16:02:44.484	-25:43:32.3076	29.33873041	6924.7062665	1.277±0.167	5.083±0.740	1.948±0.529	-	Y
203623230	8.69	16:48:53.3621	-25:30:28.5552	2.54427583	6897.2089677	0.012±0.001	2.146±0.156	0.011±0.106	-	Y
203826436	12.24	16:13:48.2426	-24:47:13.4232	6.43032491	6898.8522848	0.085±0.004	3.038±0.246	0.594±0.194	Y	Y
204129699	10.61	16:21:45.7802	-23:32:52.314	1.25783320	6896.1158511	0.716±0.024	0.931±0.018	0.366±0.028	-	Y
204346718	14.63	16:21:16.8142	-22:41:36.69	0.64292573	6896.4254449	2.460±0.070	5.977±0.147	2.299±0.128	-	-
204649811	11.61	16:19:16.9651	-21:27:36.09	2.64594828	6897.4984505	1.124±0.029	2.688±0.066	1.052±0.061	-	-
204658292	14.42	16:14:49.6498	-21:25:25.068	20.98296043	6911.5849295	0.338±0.049	2.961±0.371	0.026±0.324	-	Y
204676499	14.66	16:23:15.3377	-21:20:45.9384	1.52717920	6897.4688286	0.192±0.338, 4.28	2.298±0.177	1.149±*	-	Y
204763194	9.97	15:59:46.0469	-20:58:11.73	2.32046168	6898.0234984	0.538±0.130	2.656±0.126	1.262±0.362	-	Y
204890128	11.89	16:16:34.0346	-20:24:01.9188	12.20911650	6896.3823294	0.092±0.004	3.807±0.225	0.734±0.190	-	Y
205029914	12.18	16:36:06.065	-19:44:40.6536	4.98049071	6899.7186765	0.041±0.002	4.087±0.265	0.722±0.231	-	Y
205047565	14.65	16:40:10.489	-19:39:33.0372	14.54444130	6906.6365823	0.268±0.039	2.783±0.400	1.388±0.199	-	-
205050711	10.59	16:50:39.2681	-19:38:38.1552	4.30221683	6899.2609554	2.613±0.074	7.536±0.157	3.159±0.149	-	-
205064326	12.84	16:47:33.2239	-19:34:45.5268	8.02678456	6896.6561773	0.472±*	4.203±0.187	2.101±*	-	Y
205071984	12.01	16:49:42.2599	-19:32:34.1556	8.99002105	6900.9370741	0.344±0.014	2.757±0.285	0.029±0.281	-	Y
205145448	13.65	16:33:47.6722	-19:10:40.044	16.63091654	6902.2674888	4.087±0.058	2.255±0.080	0.488±0.074	-	-
205148699	12.39	16:52:38.5159	-19:09:41.94	4.37983009	6896.4982200	3.430±0.056	4.704±0.094	1.097±0.075	-	-
205152172	13.49	16:20:43.2019	-19:08:38.904	0.97988263	6896.5763805	0.042±0.006	1.427±0.418	0.414±0.366	-	Y
Campaign 3										

Table 3. continued.

EPIC	mag	RA	DEC	Period	T0	Depth %	T_{14} (h)	T_{12} (h)	Sec	Gr
205924614	13.09	22:15:00.4625	-17:15:02.5452	2.84947127	6983.4194982	0.372±0.005	2.093±0.060	0.429±0.051	-	-
20599468	12.93	22:21:37.5888	-14:50:22.128	12.25823207	6984.1054025	0.076±0.008	1.117±0.159	0.013±0.121	-	Y
206011496	10.92	22:48:07.566	-14:29:40.8804	2.36840828	6981.6531474	0.025±0.001	2.455±0.240	0.412±0.208	-	Y
206011691	12.32	22:41:12.8854	-14:29:20.3532	15.49412230	6988.4831011	0.121±0.009	2.210±0.340	0.391±0.299	-	Y
206026904	12.15	22:15:17.2366	-14:02:59.3088	7.05240378	6986.9773370	0.098±0.003	2.185±0.115	0.556±0.097	-	Y
206038483	12.59	22:34:25.4842	-13:43:54.1272	3.00234671	6982.0621332	0.440±0.004	3.271±0.044	0.609±0.036	-	-
206044803	12.98	22:38:41.9383	-13:33:36.0864	2.57275378	6983.2247373	0.022±0.002	2.144±0.000	0.002±0.000	-	-
206061524	14.44	22:20:13.7659	-13:06:52.6572	5.87913354	6986.3233582	0.841±0.019	2.427±0.152	0.360±0.133	-	Y
206096602	12.05	22:17:27.4032	-12:11:14.9928	6.67010938	6982.6929362	0.074±0.004	1.597±0.220	0.273±0.199	-	Y
206103150	11.76	22:04:48.7306	-12:01:08.0148	4.15810694	6982.9821510	1.142±0.021	3.798±0.089	0.868±0.072	-	-
206125618	13.89	22:09:39.2669	-11:25:43.4712	6.53147301	6986.1879749	0.072±0.006	3.167±0.543	0.387±0.475	-	Y
206144956	10.40	22:12:50.8205	-10:55:31.3536	12.65309622	6986.3216687	0.041±0.002	3.477±0.223	0.875±0.182	-	Y
206152015	11.32	22:49:21.9281	-10:44:36.3516	0.80858305	6981.7028457	1.022±0.037	2.199±0.084	1.099±0.042	-	-
206154641	11.30	22:49:32.5666	-10:40:31.9836	2.48450535	6982.6159632	0.879±0.014	1.919±0.036	0.634±0.033	-	-
206155547	14.62	22:14:25.5149	-10:39:10.026	24.39499240	6985.8779568	2.305±0.025	6.096±0.116	1.168±0.079	-	-
206175552	13.30	22:38:02.7689	-10:12:18.3852	6.57986525	6984.2148020	0.561±0.023	1.225±0.000	0.004±0.000	-	-
206181769	12.77	22:33:54.1908	-10:05:05.8056	13.98746633	6984.4318808	0.102±0.004	3.958±0.216	1.040±0.159	-	-
206245553	11.74	22:20:06.115	-9:03:21.9348	7.49491004	6987.6755418	0.058±0.001	3.830±0.135	0.600±0.111	-	-
206311743	12.92	22:20:28.4431	-8:03:37.926	4.31444335	6983.7180592	3.877±0.040	7.132±0.074	2.347±0.060	Y	-
206432863	13.01	22:28:25.3409	-6:05:12.0372	11.99899626	6983.8077715	0.701±0.017	6.656±0.212	1.780±0.163	-	-
206500801	12.19	22:17:58.1371	-4:51:52.6284	8.15306759	6985.3693350	2.292±0.038	4.477±0.083	1.206±0.066	-	-
206543223	11.49	22:24:02.6777	-3:57:15.804	17.80345864	6988.7876202	4.843±0.256	3.201±0.157	1.226±0.140	-	Y
Campaign 4										
210414957	12.65	4:17:18.0638	+13:48:17.4312	0.96997227	7062.1923191	0.549±0.017	2.191±0.037	0.943±0.049	-	Y
210448987	13.93	3:49:56.5171	+14:30:07.92	6.10099028	7064.3449682	0.077±0.005	2.378±0.278	0.528±0.232	-	Y
210472483	13.18	4:17:08.6143	+14:56:10.9608	1.14300180	7062.3070608	4.202±0.084	4.654±0.082	1.806±0.072	-	-
210508766	13.84	3:59:36.3749	+15:33:31.9896	10.00102551	7066.2663800	0.163±2967.072	3.509±0.278	1.754±*	-	Y
210512842	12.11	4:01:29.9878	+15:37:30.1332	5.86639571	7067.1524091	0.020±0.002	2.825±0.543	0.513±0.447	-	Y
210513446	13.62	3:52:04.4458	+15:38:07.0224	1.14907861	7062.4191558	2.624±0.032	1.856±0.014	0.780±0.018	-	-
210550063	11.15	4:04:31.6582	+16:13:00.0984	2.16594452	7062.8157163	0.062±357.477	2.085±0.170	1.042±6021.640	-	Y
210558622	12.03	4:03:10.2823	+16:20:50.8092	19.56614010	7064.2069310	0.135±0.002	6.227±0.116	0.955±0.089	-	-
210559259	13.70	3:57:54.205	+16:21:27.7128	14.27669647	7063.4087404	0.110±0.012	4.457±0.410	1.760±0.375	-	Y
210576234	11.60	3:35:05.4163	+16:36:55.3284	15.97700259	7071.6788591	2.990±0.014	4.926±0.019	1.982±0.017	-	-
210598340	12.54	3:47:28.4947	+16:56:29.868	3.73478175	7063.0874390	1.239±0.005	5.781±0.027	0.912±0.021	-	-
210666756	12.73	3:53:44.598	+17:53:55.9104	1.39657671	7061.9881397	0.189±0.018	1.586±0.051	0.711±0.103	-	Y
210707130	12.10	3:57:51.4546	+18:27:54.9144	0.68458757	7061.9420537	0.027±0.002	0.912±0.242	0.080±0.226	-	Y
210744674	12.89	4:23:26.1646	+19:01:38.982	25.20778830	7065.9297422	3.330±0.163	3.162±0.067	1.389±0.094	-	Y
210754505	13.19	4:18:34.7832	+19:10:44.6016	0.87052967	7062.2852757	0.182±0.020	1.502±0.085	0.623±0.126	-	Y
210769880	11.04	4:10:07.907	+19:24:40.1508	1.43689647	7062.6069667	0.124±0.114	2.367±0.148	1.162±1.137	-	Y
210843708	12.78	3:51:09.3629	+20:32:06.288	0.70416550	7062.0251688	0.117±0.265	1.775±0.109	0.885±2.027	-	Y
210877025	12.76	3:46:33.894	+21:02:03.4872	18.03895153	7071.5198711	0.121±2616.422	6.304±0.590	3.152±*	-	Y
210903662	12.05	4:00:12.2609	+21:26:51.1476	2.41040731	7063.4253439	0.563±0.008	1.847±0.030	0.666±0.028	-	-
210925707	9.52	3:48:28.9306	+21:47:50.856	1.68658840	7062.2382601	4.591±0.059	4.923±0.051	1.970±0.047	-	-
210957318	13.17	3:29:22.0709	+22:17:57.858	4.09803132	7063.8099342	1.702±0.017	2.400±0.033	0.749±0.027	-	-

Table 3. continued.

EPIC	mag	RA	DEC	Period	T0	Depth %	T_{14} (h)	T_{12} (h)	Sec	Gr
210968143	13.72	3:56:36.5772	+22:28:21.4752	13.71468745	7064.9574663	0.149±0.012	4.339±0.351	1.333±0.290	-	Y
211009047	12.54	4:04:21.4946	+23:07:04.2312	1.31982263	7062.3067288	0.213±0.032	1.588±0.387	0.476±0.344	-	Y
211048999	12.66	3:55:11.2555	+23:45:24.5052	5.17110937	7066.5875981	0.121±0.09.743	2.470±0.136	1.235±8240.485	-	Y
211077024	14.46	4:12:52.3349	+24:12:18.4032	1.41929871	7063.8737464	0.085±0.009	1.048±0.530	0.062±0.486	-	Y
211089792	12.91	4:10:40.9553	+24:24:07.3548	3.25919930	7064.4267990	1.762±0.017	2.180±0.036	0.499±0.030	-	-
211147528	11.83	3:58:35.321	+25:23:18.9204	2.34951024	7063.0590874	0.817±0.022	2.432±0.093	0.603±0.068	-	-
211169300	12.49	3:53:57.8318	+25:47:50.37	16.43831081	7067.8069350	1.529±0.009	4.389±0.024	1.462±0.020	-	-
Campaign 5										
211331236	13.90	8:55:25.3637	+10:28:08.8716	1.29162600	7142.7702712	0.146±0.014	1.381±0.427	0.204±0.387	-	Y
211342524	12.41	8:32:23.6866	+10:40:38.0604	14.45182480	7149.3614717	4.465±0.082	3.628±0.054	1.814±0.027	-	-
211355342	12.64	8:30:12.9682	+10:54:37.0584	6.89424037	7143.7947628	0.046±0.004	2.224±0.000	0.004±0.000	-	-
211359660	11.74	8:40:43.2785	+10:58:58.5876	4.73730765	7145.9396599	0.115±0.002	2.833±0.077	0.627±0.063	-	-
211383821	14.04	8:44:09.925	+11:23:07.8072	1.56706496	7143.2883485	0.049±198.308	2.144±0.283	1.072±4337.749	-	Y
211391664	12.10	8:25:57.1894	+11:30:40.122	10.13892836	7145.9770277	0.095±0.002	5.371±0.197	0.803±0.154	-	-
211399359	14.42	8:32:16.1141	+11:37:50.6172	3.11491262	7144.5317227	2.698±0.014	2.375±0.022	0.532±0.018	-	-
211413752	13.54	8:54:50.2908	+11:50:53.754	9.33155684	7150.1895459	0.134±1426.191	3.950±0.474	1.975±*	-	Y
211418729	14.29	8:31:31.9109	+11:55:20.154	11.38576954	7151.7225250	1.470±0.062	4.390±0.193	1.491±0.163	-	-
211432103	10.25	8:55:24.594	+12:07:35.9616	0.93346092	7142.1730638	0.194±0.581	2.338±0.227	1.163±3.550	-	Y
211442297	13.19	8:26:12.8266	+12:16:54.9696	20.27362337	7157.1552156	1.666±0.016	3.671±0.081	0.825±0.051	-	-
211492449	14.28	8:43:45.2225	+13:01:49.5696	16.24196986	7149.8870397	0.241±0.080	4.391±0.540	2.024±0.917	-	Y
211525389	11.69	8:21:40.8665	+13:29:51.108	8.26345949	7148.0030800	0.129±0.003	3.704±0.140	0.694±0.112	-	-
211529065	13.43	8:45:03.9833	+13:32:59.3988	4.39883617	7142.9862785	0.132±0.006	1.980±0.148	0.544±0.125	-	Y
211541590	14.34	9:08:42.4639	+13:43:27.4368	9.81881482	7143.3869711	0.285±0.056	3.206±0.505	1.298±0.465	-	Y
211562654	12.75	8:20:01.7184	+14:01:10.0596	10.79305290	7147.7736526	0.068±0.004	3.942±0.362	1.037±0.268	Y	Y
211572511	11.69	8:26:05.2231	+14:09:26.0784	10.39528014	7152.2705607	0.019±0.003	4.442±0.809	1.354±0.691	-	Y
211578235	14.33	9:00:14.7446	+14:14:15.216	11.00357542	7147.9869470	0.780±1.721	1.503±0.133	0.743±1.687	-	Y
211579683	14.03	8:20:51.492	+14:15:31.1976	9.01258853	7144.6142532	0.081±0.008	3.639±0.557	0.585±0.455	-	Y
211594205	10.68	8:36:33.6257	+14:27:42.9696	16.99291698	7148.5005008	0.037±0.001	2.719±0.201	0.525±0.158	-	Y
211682423	12.62	8:48:22.2487	+15:40:44.0796	6.96350934	7148.7282635	0.016±0.003	2.189±0.000	0.001±0.000	-	-
211713099	13.64	8:20:53.7314	+16:05:27.4092	8.56394776	7149.7095696	0.524±0.012	3.510±0.098	0.842±0.079	-	-
211719484	12.56	8:13:55.6536	+16:10:41.0376	0.36091387	7142.5176386	0.739±9192.391	1.692±0.015	0.846±*	-	Y
211731298	13.04	8:36:09.889	+16:20:37.2948	1.99067602	7143.3286981	0.034±0.003	1.862±0.436	0.039±0.415	-	Y
211733267	12.15	8:40:02.2591	+16:22:20.6616	8.65871336	7144.9299968	0.873±*	1.560±0.097	0.780±*	-	Y
211736671	12.16	8:13:31.65	+16:25:10.5924	4.73360988	7145.0950979	0.083±0.002	3.605±0.192	0.508±0.163	-	Y
211754962	13.94	8:16:07.0738	+16:40:37.7868	3.41052823	7145.2701113	0.060±631.502	2.124±0.308	1.062±*	-	Y
211770795	14.49	8:48:02.3362	+16:54:06.6708	7.72651124	7148.8315481	0.087±0.014	3.199±0.441	1.195±0.446	-	Y
211784767	11.85	8:24:03.3142	+17:05:56.454	3.57804902	7143.7896753	0.008±0.001	4.905±0.723	1.038±0.601	Y	Y
211791178	13.65	8:48:34.3171	+17:11:26.4696	9.56332821	7146.9103516	0.076±0.007	3.039±0.551	0.264±0.515	-	Y
211796070	13.94	8:33:14.6573	+17:15:41.6268	1.89016107	7142.6188451	0.027±0.004	2.224±0.412	1.112±0.206	-	-
211797637	13.71	8:42:55.5024	+17:16:58.2312	1.64117466	7143.0644401	0.020±0.002	1.337±0.047	0.001±0.030	-	Y
211800191	12.44	8:51:32.3477	+17:19:11.4024	1.10605213	7142.9669265	0.147±0.020	1.289±0.054	0.555±0.117	-	Y
211804579	11.22	8:36:16.2662	+17:22:53.9796	1.52317871	7142.7274735	0.734±0.013	4.004±0.054	1.651±0.051	Y	-
211808055	13.74	8:36:08.2706	+17:25:48.2952	3.38199819	7142.6125147	0.339±0.010	5.484±0.106	2.381±0.108	-	-
211816003	13.65	8:50:29.0688	+17:32:32.802	14.45182127	7144.8604659	0.118±0.005	3.220±0.037	0.005±0.025	-	Y

Table 3. continued.

EPIC	mag	RA	DEC	Period	T0	Depth %	T_{14} (h)	T_{12} (h)	Sec	Gr
211818569	12.94	8:27:44.8128	+17:34:45.8292	5.18597200	7143.5609706	1.263±0.009	2.148±0.027	0.512±0.022	-	-
211822797	14.57	8:41:38.4876	+17:38:24.018	21.17623917	7144.4194340	0.071±0.013	2.008±1.203	0.248±1.040	-	Y
211825866	13.78	8:17:19.8636	+17:41:02.1948	0.95017067	7142.6157733	0.088±348.370	2.581±0.127	1.291±5103.590	-	Y
211886472	11.13	9:08:31.8074	+18:31:42.7548	19.63366256	7152.3879588	0.682±*	2.331±0.204	1.164±*	-	Y
211913977	12.62	8:41:22.5804	+18:56:01.95	14.66146147	7152.7158442	0.072±0.007	5.347±0.435	2.252±0.382	Y	Y
211919004	13.13	8:39:06.4913	+19:00:36.0828	11.71571445	7149.1066172	0.111±0.004	4.358±0.491	0.056±0.485	-	Y
211925595	14.47	8:51:49.9512	+19:06:27.108	45.38331501	7143.1611934	0.229±0.027	5.429±0.601	2.148±0.521	-	Y
211929937	14.16	8:36:42.829	+19:10:25.7232	3.47701312	7142.4106520	2.062±0.012	2.646±0.024	0.600±0.020	-	-
211945201	10.11	9:06:17.754	+19:24:08.1072	19.50735025	7158.8217047	0.150±0.008	3.951±0.303	1.061±0.235	-	Y
211987231	11.68	9:09:31.9171	+20:02:53.682	17.04066667	7158.8429345	1.938±0.170	2.260±0.208	0.864±0.194	-	Y
211990866	10.41	8:38:24.3	+20:06:21.8268	1.67344228	7142.3952529	0.086±2096.429	2.125±0.278	1.062±*	-	Y
212006344	12.47	8:25:54.3146	+20:21:34.4484	2.21944122	7144.0480533	0.040±0.004	1.533±0.245	0.423±0.221	-	Y
212008766	12.80	8:37:07.7851	+20:23:57.7428	14.11544241	7145.1494125	0.083±0.006	4.192±0.359	1.222±0.273	-	Y
212012119	11.75	8:48:40.7748	+20:27:18.2736	3.28046294	7142.1379804	0.083±0.004	2.264±0.175	0.621±0.145	-	Y
212066407	12.18	8:39:21.2438	+21:23:26.9844	0.82182448	7142.8327854	0.047±0.002	0.691±0.004	0.001±0.000	Y	-
212069861	14.10	8:57:46.6054	+21:27:12.7188	30.96028326	7147.4866566	0.202±0.013	4.117±0.326	0.932±0.283	-	Y
212099230	10.51	8:32:17.657	+22:00:21.6396	7.11047482	7149.0798796	0.070±0.002	3.434±0.106	1.149±0.086	-	-
212110007	14.24	8:53:14.635	+22:13:08.3172	16.70043510	7144.7000570	3.552±0.298	3.240±0.263	1.222±0.236	-	Y
212110888	11.44	8:30:18.9048	+22:14:09.2688	2.99529334	7144.3485727	0.731±0.006	2.475±0.027	0.673±0.022	-	-
212133517	13.39	8:24:41.8862	+22:41:20.1588	9.73605539	7151.1609617	0.122±0.022	3.673±0.548	1.086±0.506	-	Y
212150006	14.70	8:32:40.6906	+23:01:55.1964	0.89803906	7142.6837188	0.163±0.029	1.611±0.144	0.653±0.211	-	Y
212157262	12.86	8:50:05.6662	+23:11:33.3636	7.15451552	7146.3132819	0.097±0.004	2.514±0.000	0.004±0.000	-	-
212164470	12.70	8:39:15.2714	+23:21:26.9316	7.81110453	7144.8598225	0.034±0.004	3.433±0.780	0.458±0.684	-	Y
Campaign 6										
212294561	13.15	13:40:35.305	-17:41:42.9756	2.76294135	7226.1094075	0.052±0.006	2.758±0.310	1.379±0.155	-	-
212300977	11.74	13:35:01.9464	-17:30:12.78	4.46659676	7229.4554874	1.529±0.035	3.480±0.154	0.438±0.134	-	Y
212315941	14.41	13:32:20.9434	-17:03:40.2912	12.93488160	7226.5563699	1.516±0.031	2.064±0.050	0.774±0.042	-	-
212351026	14.54	13:26:44.8493	-16:06:18.54	2.55068936	7225.7853107	0.828±0.027	7.155±0.240	2.961±0.188	Y	-
212351405	13.99	13:26:39.1049	-16:05:42.0036	2.55234671	7225.7532124	0.630±0.019	5.966±0.266	1.647±0.210	Y	-
212357477	10.22	13:28:03.9919	-15:56:16.152	6.32976960	7227.5459738	0.042±0.003	2.486±0.219	0.703±0.178	-	Y
212394689	12.21	13:34:29.1113	-15:02:10.8924	6.67773603	7230.1047856	0.066±0.003	2.986±0.235	0.526±0.192	Y	Y
212425103	14.49	13:37:28.7014	-14:20:56.0004	0.94599529	7225.7417902	0.028±0.004	1.703±0.763	0.259±0.665	-	Y
212435047	12.39	13:28:31.3721	-14:07:34.6512	1.11562824	7225.1363478	0.017±0.001	1.161±0.029	0.003±0.027	-	Y
212460519	12.44	13:34:11.1698	-13:34:36.9408	7.38795716	7231.1788397	0.077±0.004	2.751±0.219	0.507±0.184	-	Y
212496592	12.97	13:26:33.4006	-12:48:23.6448	2.85794855	7225.2786951	0.026±0.003	2.799±0.335	0.893±0.286	-	Y
212521166	11.59	13:49:23.8896	-12:17:04.1676	13.85870316	7233.7474506	0.126±0.004	3.747±0.137	0.910±0.109	-	-
212530118	13.56	13:31:35.5942	-12:05:42.3384	12.83724862	7230.1279057	0.054±0.011	3.944±0.496	1.666±0.531	-	Y
212543933	14.01	13:46:36.5575	-11:48:17.7948	7.80651068	7231.3008817	0.053±0.009	3.200±0.540	1.218±0.523	-	Y
212570977	13.93	13:43:36.3341	-11:13:24.852	8.85007649	7232.7576032	2.597±0.040	4.384±0.105	1.056±0.075	-	-
212572439	12.84	13:37:45.6173	-11:11:33.2664	2.58166013	7225.6078290	0.499±0.008	1.911±0.051	0.531±0.042	-	-
212577658	11.54	13:55:00.8054	-11:04:47.3556	14.07277587	7235.3808180	0.040±0.001	3.004±0.258	0.389±0.230	-	Y
212585579	12.63	13:39:15.7853	-10:54:25.1172	3.02164122	7227.6099015	0.149±879.613	1.736±0.059	0.868±5124.267	-	Y
212587672	12.19	13:41:46.7299	-10:51:44.7552	23.24110566	7237.0305094	0.069±569.265	4.505±0.404	2.252±*	-	Y
212601505	14.49	13:30:33.9974	-10:33:19.3968	0.72436144	7225.1158941	3.564±2.573	1.238±0.043	0.613±0.460	-	Y

Table 3. continued.

EPIC	mag	RA	DEC	Period	T0	Depth %	T_{14} (h)	T_{12} (h)	Sec	Gr
212645891	12.64	14:01:05.5248	-9:32:24.4032	0.32814902	7225.2597894	0.235±0.017	1.006±0.035	0.419±0.060	-	Y
212661144	13.60	13:56:56.0014	-9:11:15.4572	2.45840745	7226.2937810	0.063±0.006	1.097±0.078	0.005±0.085	-	Y
212697709	12.19	13:26:37.2461	-8:19:03.216	3.95169560	7226.1902326	0.750±0.005	1.853±0.020	0.585±0.017	-	-
212705192	11.73	13:30:25.3042	-8:07:48.9432	2.26884990	7226.4170802	0.779±*	2.475±0.068	1.237±*	-	Y
212735333	11.98	13:29:34.4806	-7:22:26.4072	8.35470947	7226.5534182	0.055±0.003	3.863±0.232	0.767±0.202	Y	Y
212737443	14.46	13:36:53.2075	-7:19:05.3184	13.60697954	7234.9532932	0.146±0.016	3.498±0.370	1.163±0.365	-	Y
212756297	13.01	13:50:37.4076	-6:48:14.4144	1.33711405	7226.1328529	3.217±0.006	1.844±0.006	0.447±0.005	-	-

Table 5. Parameters for the ebs candidates.

EPIC	mag	RA	DEC	Period	T0	Depth %	T_{14} (h)	T_{12} (h)	Sec	Gr
Campaign 1										
201158453	14.69	11:35:55.3694	-5:05:37.95	7.07626177	6813.4862974	11.154±0.128	4.504±0.041	1.781±0.038	-	-
201160662	12.12	11:39:59.4691	-5:02:24.846	1.53717783	6818.1794506	1.383±0.060	7.303±0.323	3.652±0.161	Y	-
201184068	14.14	11:33:59.3158	-4:28:47.7984	1.58860603	6813.7522849	62.967±533.617	2.326±0.012	1.163±*	Y	Y
201193666	14.62	11:16:07.2293	-4:15:01.764	0.43292816	6813.7583017	23.912±0.681	1.198±0.081	0.277±0.074	Y	Y
201253025	12.86	11:57:19.8415	-3:09:42.588	6.78657519	6823.9778149	25.671±0.078	5.954±0.013	2.558±0.013	Y	-
201306196	12.73	11:59:32.0326	-2:21:27.2808	7.25648360	6819.7306604	0.528±0.019	2.863±0.077	1.130±0.083	Y	-
201382417	11.66	11:20:38.3957	-1:13:33.4668	5.19784929	6821.4691946	7.038±0.037	4.812±0.027	1.668±0.021	Y	-
201382958	13.53	11:13:57.6974	-1:13:05.4372	3.20531346	6818.2532917	21.661±0.138	6.436±0.049	1.847±0.037	Y	-
201390608	13.36	11:33:37.9114	-1:06:12.5352	9.81161598	6822.3852228	14.625±0.129	3.767±0.041	1.147±0.032	Y	-
201407812	11.86	11:36:10.5948	-0:50:26.5164	2.82621695	6815.3250016	13.914±0.090	6.258±0.032	2.564±0.029	-	-
201408204	11.85	11:30:03.2402	-0:50:03.9228	8.48220256	6818.4957840	41.788±0.528	5.260±0.034	2.426±0.042	Y	-
201458798	12.09	11:13:07.2358	-0:05:33.0648	0.61941709	6813.0299113	21.494±0.395	1.913±0.027	0.770±0.030	Y	-
201460467	14.27	11:49:34.1532	-0:04:05.2176	1.06624664	6813.3080223	18.961±0.437	1.695±0.058	0.528±0.052	-	-
201473612	13.14	11:09:08.3256	+0:07:31.9188	1.37171460	6814.2375111	64.314±0.333	5.756±0.029	2.441±0.023	Y	-
201488365	8.81	11:12:45.095	+0:20:52.8324	3.36441050	6815.5860492	35.598±0.116	6.727±0.017	2.959±0.016	-	-
201523873	13.84	11:31:04.1614	+0:53:26.2824	1.24046862	6818.6909605	20.877±0.228	2.345±0.018	0.985±0.020	Y	-
201530296	13.77	11:36:52.5497	+0:59:28.2192	10.34265104	6814.2978785	48.881±11.553	3.088±0.019	1.543±0.368	-	Y
201567796	12.36	11:28:41.8195	+1:33:06.912	5.00873881	6822.5828664	4.409±0.011	4.844±0.014	0.963±0.012	Y	-
201569483	11.77	11:08:41.1118	+1:34:39.0468	5.79586612	6813.3198782	9.256±0.186	2.381±0.045	0.924±0.042	-	-
201576812	10.07	11:46:10.2127	+1:41:15.1296	5.72773921	6820.3284912	12.381±0.404	3.109±0.080	1.258±0.078	Y	-
201594823	12.14	11:09:20.1509	+1:57:49.7808	1.30068256	6818.7707455	31.660±0.196	2.730±0.018	1.017±0.015	Y	-
201607088	14.25	11:23:55.3361	+2:09:11.7144	0.53092719	6813.5279106	18.793±0.460	1.884±0.029	0.792±0.037	Y	-
201637354	12.33	11:21:41.2267	+2:37:19.0848	3.38759456	6818.6056957	43.211±0.155	8.740±0.031	3.583±0.024	Y	-
201648133	10.14	11:11:33.4632	+2:47:13.3476	34.98894834	6848.8011581	37.386±2.026	9.097±0.402	4.069±0.348	-	Y
201649426	13.22	11:48:56.2229	+2:48:27.4284	55.57865694	6821.3255648	9.439±1.001	3.739±0.379	1.870±0.190	Y	-
201665500	12.14	11:49:37.7242	+3:04:01.7616	3.05333870	6819.6996248	6.734±0.017	3.921±0.014	0.880±0.011	Y	-
201677835	14.02	11:44:29.6508	+3:16:20.73	20.52067414	6817.4670079	0.095±0.015	4.046±0.618	1.561±0.514	Y	Y
201680569	13.76	11:34:04.6193	+3:18:57.2832	0.78475697	6818.7356817	34.672±0.338	1.991±0.014	0.838±0.016	Y	-
201695625	12.92	12:04:54.7843	+3:33:56.2644	0.58436368	6818.5787934	11.642±0.366	3.079±0.124	0.858±0.100	Y	-
201715262	11.37	12:03:12.7296	+3:54:00.1008	1.05399502	6818.8884811	21.278±0.126	6.042±0.030	2.491±0.026	-	-
201720463	13.95	11:25:24.8678	+3:59:14.694	3.55718571	6819.4478914	8.438±0.110	4.822±0.082	1.078±0.064	Y	-
201725399	12.30	11:13:43.3642	+4:04:22.476	2.16115302	6819.9104348	35.457±0.267	6.939±0.040	2.986±0.036	Y	-
201749821	12.95	11:22:25.7352	+4:28:49.3572	1.40190154	6819.1601031	31.102±0.197	5.848±0.037	2.213±0.030	Y	-
2018900494	12.02	11:50:58.7731	+7:07:29.4348	2.53734743	6820.5829552	11.428±0.236	2.819±0.043	1.177±0.044	Y	-
201893576	13.60	11:26:49.0728	+7:11:17.9664	0.92975055	6818.5637604	8.158±*	1.593±0.012	0.796±*	Y	Y
201921381	13.82	11:40:32.2565	+7:46:59.0664	0.56024517	6818.1015578	11.894±0.553	2.245±0.060	0.931±0.075	Y	Y
Campaign 2										
202627452	9.85	16:09:44.0887	-28:57:47.826	2.49322870	6897.4774947	0.213±0.015	2.280±0.149	0.840±0.155	Y	Y
202627721	9.90	16:09:44.0282	-28:57:44.2152	2.49322870	6897.4776186	0.216±0.015	2.302±0.149	0.856±0.156	Y	Y
202643279	12.25	16:34:17.8349	-28:54:12.78	2.34348254	6898.1082878	8.030±0.110	5.122±0.064	2.022±0.055	Y	-
202685083	11.45	16:16:17.2546	-28:44:42.5148	3.32382042	6898.7163126	86.863±0.302	9.527±0.059	3.503±0.037	Y	-
202733088	11.20	16:44:24.3151	-28:33:57.3084	1.71558325	6897.4178604	22.470±0.315	7.252±0.062	3.192±0.067	Y	-
202828096	10.98	16:39:02.8421	-28:12:56.7828	1.43607494	6897.4385791	39.249±0.662	3.649±0.039	1.613±0.044	Y	-

Table 5. continued.

EPIC	mag	RA	DEC	Period	T0	Depth %	T_{14} (h)	T_{12} (h)	Sec	Gr
202843107	11.83	16:22:11.4689	-28:09:42.5628	2.19902451	6896.4931113	33.158±0.312	6.180±0.036	2.805±0.038	-	-
202844711	12.36	16:18:47.9042	-28:09:21.0456	6.17849322	6897.4258633	13.422±0.138	7.490±0.069	2.902±0.057	Y	-
202963882	13.82	16:13:18.905	-27:44:02.4792	0.63072595	6896.3863624	8.264±0.287	1.994±0.051	0.795±0.058	Y	Y
203060993	12.55	16:43:57.9156	-27:23:35.7972	5.95807340	6897.9224431	22.658±0.382	5.776±0.096	2.303±0.082	Y	-
203361171	11.92	15:56:02.9806	-26:23:54.7872	7.31837950	6898.0835961	9.752±0.182	6.010±0.113	2.342±0.088	Y	-
203371239	11.74	16:16:39.3828	-26:21:55.7892	10.18026735	6901.8018922	27.207±0.967	8.500±0.189	3.394±0.180	-	-
203463506	13.02	16:03:36.3074	-26:03:12.8268	0.69587488	6896.1480037	40.624±1.290	3.412±0.050	1.563±0.071	Y	Y
203476597	9.57	16:25:57.9154	-26:00:37.3536	0.72028611	6896.5426833	3.745±*	2.890±0.109	1.445±*	Y	Y
203485624	12.35	16:16:41.2927	-25:58:49.8756	0.84129444	6896.2629951	20.033±0.448	4.356±0.111	1.432±0.088	Y	-
203633064	12.30	15:56:54.1147	-25:28:25.8888	0.70994967	6896.2529625	1.795±0.113	1.986±0.031	0.924±0.077	Y	Y
203636784	12.87	16:01:05.2764	-25:27:38.9484	6.76024678	6899.5584431	22.266±0.466	5.473±0.102	1.978±0.086	Y	-
203637922	14.27	16:23:58.8986	-25:27:24.8112	4.30560750	6896.2270421	27.256±0.344	5.572±0.051	2.400±0.049	Y	-
203710387	14.27	16:16:30.683	-25:12:20.1708	1.40451281	6896.1158230	6.857±0.186	2.197±0.053	0.831±0.052	-	-
203749579	14.50	16:30:08.4098	-25:04:04.3068	0.47749922	6896.0862159	17.989±0.330	3.377±0.050	1.298±0.047	-	-
203868608	13.32	16:17:18.9869	-24:37:18.6564	4.54062462	6896.2044171	13.551±0.302	2.737±0.071	1.368±0.036	Y	-
203878683	10.46	16:07:44.3554	-24:34:51.96	13.75238652	6905.2991622	9.931±0.463	6.368±0.341	2.367±0.247	Y	Y
203929178	11.16	16:49:41.4518	-24:22:25.7088	1.15387912	6897.0430167	6.032±0.118	3.291±0.056	1.291±0.052	-	-
203936580	12.47	16:49:36.109	-24:20:33.594	1.20749577	6896.7810345	0.421±*	2.112±0.060	1.056±*	Y	Y
203942067	12.08	16:15:17.873	-24:19:09.2208	1.64034684	6897.1784345	14.163±0.214	3.655±0.048	1.470±0.043	-	-
204073447	11.71	16:13:47.9717	-23:46:26.7204	3.25087900	6896.5188616	4.385±0.093	2.780±0.063	1.040±0.055	Y	-
204165788	7.28	16:25:35.0822	-23:24:18.7668	0.74722612	6896.1425435	0.180±0.011	2.198±0.545	0.131±0.520	Y	Y
204193529	11.03	15:56:11.7127	-23:17:48.3	5.50199176	6899.9269045	16.661±0.045	4.185±0.013	1.409±0.010	Y	-
204275121	12.98	16:28:58.8379	-22:58:38.8272	2.19420304	6897.9845503	18.502±0.219	5.275±0.052	2.103±0.047	Y	-
204321014	12.43	15:57:53.4485	-22:47:45.3444	3.79273116	6897.8491321	42.171±0.310	4.058±0.018	1.829±0.021	Y	-
204411840	9.35	16:13:57.2474	-22:26:20.49	3.99237018	6896.9974280	9.808±0.210	7.382±0.136	2.910±0.113	Y	-
204470067	14.30	16:40:56.8373	-22:12:32.4792	1.84720163	6897.7577533	14.070±0.236	2.160±0.031	0.858±0.032	Y	-
204498681	12.74	16:01:03.4025	-22:05:35.9736	5.53684685	6898.7361626	0.287±0.018	3.475±0.198	1.419±0.169	-	Y
204531124	12.14	16:00:51.438	-21:57:32.1588	3.43125652	6897.4594314	1.497±0.029	2.225±0.040	0.865±0.037	Y	-
204538021	10.85	16:04:03.1632	-21:55:49.3212	0.91472713	6896.1608863	3.481±4.064	1.930±0.085	0.959±1.145	Y	Y
204538608	8.69	16:04:02.8349	-21:55:40.1484	0.91491864	6896.1560393	28.789±0.466	2.160±0.026	0.901±0.029	Y	-
204561871	12.71	15:58:46.5737	-21:49:48.2196	2.36184773	6897.6503719	71.362±0.407	7.578±0.040	3.353±0.033	Y	-
204576757	13.67	16:28:37.8259	-21:46:03.018	23.27384132	6898.0908315	19.321±0.185	4.178±0.047	1.623±0.035	-	-
204596569	11.81	16:20:48.383	-21:41:03.7104	2.29046164	6897.1407819	0.220±0.005	1.923±0.046	0.961±0.023	Y	-
204676803	11.92	16:23:16.7916	-21:20:41.4528	1.52722342	6897.4688695	11.315±0.066	2.871±0.024	0.824±0.018	Y	-
204676841	11.98	16:23:16.9346	-21:20:40.9056	1.52722342	6897.4688725	11.393±0.038	2.834±0.014	0.775±0.011	Y	-
204753706	11.84	15:56:14.8865	-21:00:40.9068	1.01895212	6896.3675072	27.960±0.397	2.375±0.024	0.988±0.027	Y	-
204760247	5.95	15:57:40.464	-20:58:59.0952	4.59876018	6898.9690844	19.291±0.763	7.075±0.236	2.830±0.206	-	-
204824945	11.13	16:13:20.227	-20:41:40.4232	1.28325753	6897.2819491	5.447±0.107	4.366±0.086	1.481±0.071	Y	-
204873331	12.34	16:38:13.2007	-20:28:34.6944	1.31815881	6896.7697419	2.097±3.347	2.213±0.114	1.099±1.797	Y	Y
204942752	12.16	16:09:04.9174	-20:09:23.976	2.48025738	6896.5647976	0.753±0.011	4.805±0.067	1.821±0.056	-	-
205046529	13.73	16:10:26.387	-19:39:51.0552	1.83466430	6896.3182840	0.867±0.047	4.753±0.278	1.386±0.219	Y	Y
205068000	12.62	16:02:36.1589	-19:33:42.8148	0.68604295	6896.0582592	0.215±2.194.070	1.724±0.065	0.862±8776.836	Y	Y
205129673	13.66	15:54:40.3978	-19:15:26.4996	0.95504168	6896.5057808	54.559±0.515	3.967±0.027	1.726±0.027	Y	-
205131464	12.32	16:20:01.74	-19:14:54.402	1.55466085	6897.4092763	16.473±0.146	5.564±0.038	2.317±0.036	Y	-

Table 5. continued.

EPIC	mag	RA	DEC	Period	T0	Depth %	T_{14} (h)	T_{12} (h)	Sec	Gr
205146590	11.06	16:45:02.1274	-19:10:20.19	1.34259216	6896.2998972	11.655±0.075	4.710±0.023	1.941±0.022	-	-
205167843	11.82	16:50:23.3424	-19:03:52.0128	1.63390713	6896.0626317	46.231±0.385	5.568±0.036	2.361±0.033	Y	-
205377483	12.62	16:09:16.0003	-17:56:36.762	0.78764200	6896.3562230	0.051±0.034	1.062±0.209	0.477±0.478	Y	Y
205463986	10.92	16:06:06.6326	-17:25:02.478	2.32437005	6898.2338769	15.096±0.181	3.703±0.034	1.530±0.033	-	-
205483258	13.72	16:23:24.5465	-17:17:27.1248	5.66484295	6896.1372139	9.637±0.416	6.309±0.180	2.738±0.184	Y	Y
205506785	8.39	16:08:17.0136	-17:08:05.3088	1.75814613	6897.8201258	3.424±0.155	5.529±0.212	2.230±0.186	Y	Y
205554809	10.57	16:09:08.4775	-16:48:10.0476	4.09461717	6896.5032749	3.158±0.018	3.723±0.020	1.426±0.017	Y	-
205684800	10.98	16:18:55.5163	-15:48:16.11	3.11375261	6897.4052924	1.981±0.047	2.803±0.060	1.088±0.057	Y	-
205703649	12.49	16:29:22.2461	-15:38:30.3648	4.05535302	6899.9116843	6.968±0.192	6.964±0.151	2.792±0.134	-	-
205728169	13.64	16:32:33.9007	-15:25:14.862	1.78860871	6897.8605194	37.935±0.845	5.812±0.119	1.876±0.101	Y	-
Campaign 3										
205919993	10.14	22:26:58.7071	-17:25:28.0236	11.00354925	6988.5527860	5.015±0.323	2.426±0.140	0.946±0.131	-	Y
205945953	12.98	22:30:34.9877	-16:30:12.9744	0.94222607	6981.9357807	46.689±0.416	4.849±0.041	1.985±0.035	Y	-
205962262	12.50	22:45:11.844	-15:58:18.462	0.84989823	6981.7717882	14.197±0.113	2.559±0.027	0.724±0.023	Y	-
205962680	9.44	22:40:08.124	-15:57:31.554	1.88216895	6981.6122938	5.338±0.060	4.201±0.036	1.718±0.034	Y	-
205968100	10.82	22:40:34.0301	-15:47:20.67	0.51364744	6981.2295591	10.991±0.302	3.069±0.073	1.180±0.068	-	-
205978103	13.73	22:28:42.7565	-15:28:43.3668	0.64290283	6981.1018987	31.352±0.630	1.937±0.022	0.828±0.030	Y	-
205982900	10.23	22:23:15.9302	-15:19:56.208	6.72058569	6983.7434194	42.022±0.181	6.785±0.020	3.018±0.020	Y	-
205985357	13.59	22:26:05.7302	-15:15:34.3116	4.13537721	6981.6878077	6.589±0.183	8.105±0.204	2.937±0.165	Y	-
206019504	14.50	22:32:12.0089	-14:15:37.9872	4.85503576	6981.7420578	14.327±0.140	2.051±0.018	0.799±0.018	Y	-
206036749	13.01	22:09:54.299	-13:46:39.72	1.13129441	6982.1207546	0.109±0.012	0.960±0.198	0.199±0.198	Y	Y
206038285	12.85	22:07:02.388	-13:44:11.7276	2.04089232	6981.2638555	24.061±0.467	5.339±0.084	2.215±0.076	Y	-
206049101	12.76	22:19:21.5318	-13:26:46.0824	0.70367753	6981.7541809	13.460±*	3.455±0.060	1.728±*	Y	Y
206049222	11.73	22:19:21.2813	-13:26:33.7164	0.70375026	6981.7518718	12.795±0.688	3.448±0.062	1.610±0.112	Y	Y
206066442	12.65	22:07:49.0608	-12:58:49.4616	1.05422160	6981.4162423	5.429±0.193	1.731±0.053	0.663±0.058	Y	Y
206066862	10.28	22:35:26.6522	-12:58:10.0992	11.08716751	6988.9166628	13.145±0.112	3.704±0.024	1.510±0.024	Y	-
206066909	12.37	22:30:49.2055	-12:58:05.9916	12.94170567	6982.0619722	19.492±0.545	4.336±0.114	1.532±0.095	-	-
206067723	11.68	22:52:04.0632	-12:56:47.3568	1.04430423	6981.4328849	38.644±0.526	4.289±0.035	1.925±0.040	Y	-
206067769	9.85	22:52:03.8839	-12:56:43.6596	1.04494532	6981.4146673	39.309±0.431	4.227±0.028	1.885±0.032	Y	-
206081536	13.46	21:58:07.009	-12:34:47.5536	0.35729157	6981.4075432	42.980±870.092	2.382±0.016	1.191±*	-	Y
206100943	9.76	22:03:45.0984	-12:04:31.9764	1.60111162	6981.5526903	1.097±0.021	1.760±0.029	0.693±0.032	Y	-
206109113	13.59	22:05:13.5158	-11:52:15.6792	1.32392166	6982.1212393	4.178±0.069	1.793±0.035	0.896±0.017	Y	-
206134477	12.14	22:53:24.2129	-11:11:52.7568	2.11814035	6981.4227272	36.856±0.184	6.322±0.023	2.792±0.023	-	-
206135267	9.23	22:13:10.7474	-11:10:38.4888	2.57340205	6982.6207794	4.986±0.125	2.702±0.078	0.888±0.064	Y	-
206139574	14.62	22:10:53.2512	-11:03:53.1936	0.67307005	6981.0756045	21.881±0.212	1.831±0.016	0.714±0.017	Y	-
206143957	11.82	22:12:45.3521	-10:57:03.9132	4.24729169	6983.4587874	27.365±0.230	5.186±0.032	2.239±0.030	Y	-
206159239	12.16	22:36:32.6042	-10:33:44.172	0.92431813	6981.5899081	26.657±0.358	3.466±0.041	1.402±0.038	Y	-
206173295	13.00	22:36:00.8261	-10:15:02.4336	2.17567216	6982.9591336	2.504±0.086	2.425±0.081	0.901±0.075	Y	-
206187484	11.41	22:18:41.1607	-9:58:32.0196	3.65184547	6983.1283202	13.475±0.131	3.349±0.031	1.341±0.027	Y	-
206226010	12.96	22:03:45.9826	-9:20:52.5192	6.91628912	6983.4053030	5.523±0.080	3.222±0.045	1.194±0.040	Y	-
206259533	10.93	22:14:46.8785	-8:50:45.726	0.96725715	6982.0095218	7.623±0.333	5.153±0.169	2.114±0.161	Y	Y
206260730	11.91	22:05:00.8414	-8:49:39.9468	2.05920404	6981.6903083	82.989±0.223	6.094±0.018	2.671±0.014	Y	-
206268154	12.54	22:05:39.9655	-8:42:59.6376	1.08094494	6982.1291120	57.208±0.341	3.946±0.016	1.775±0.017	Y	-
206288770	12.45	22:17:03.8558	-8:24:47.0016	24.77972612	6993.0177274	18.416±0.776	6.052±0.240	2.460±0.199	-	Y

Table 5. continued.

EPIC	mag	RA	DEC	Period	T0	Depth %	T_{14} (h)	T_{12} (h)	Sec	Gr
206314138	10.84	22:09:45.7363	-8:01:21.3168	2.07510313	6983.0744438	3.434±0.105	3.190±0.090	1.264±0.081	Y	-
206380678	13.57	22:03:11.5361	-6:56:34.6848	4.53943379	6982.5571367	0.519±0.022	1.903±0.108	0.601±0.095	Y	Y
206412289	14.61	22:10:58.9356	-6:25:48.4716	3.30694818	6981.7890220	18.457±0.252	2.391±0.032	0.953±0.029	Y	-
206477939	12.07	22:42:57.1889	-5:18:38.79	2.68544015	6983.2270375	7.147±0.104	1.990±0.031	0.995±0.016	Y	-
206489474	13.65	22:39:19.0099	-5:05:23.8128	1.51703847	6982.4322245	8.272±0.058	1.878±0.015	0.939±0.007	Y	-
206532093	11.56	22:22:18.6967	-4:12:22.6008	2.20217816	6981.7897762	28.560±0.228	5.691±0.033	2.409±0.032	Y	-
Campaign 4										
210370729	11.48	3:52:58.3416	+12:46:04.26	1.08594477	7062.4153547	14.725±0.285	3.434±0.047	1.441±0.049	Y	-
210375290	10.96	3:57:43.4678	+12:52:42.132	2.41764727	7063.8855080	12.788±0.118	4.115±0.046	1.219±0.036	Y	-
210386880	11.03	3:45:34.3097	+13:09:33.0804	7.21557656	7068.9510781	36.296±0.341	3.266±0.037	1.633±0.019	Y	-
210401157	10.42	3:57:27.9072	+13:29:37.3308	1.31558265	7062.0220229	4.050±0.086	2.299±0.039	0.916±0.040	Y	-
210403086	11.11	3:38:56.401	+13:32:21.8796	2.25443154	7062.8709134	41.055±0.194	6.707±0.028	2.788±0.024	Y	-
210404228	13.15	4:10:53.3602	+13:33:54.1584	1.12004904	7062.9107657	7.854±*	2.893±0.020	1.447±*	Y	Y
210434247	12.49	3:36:52.2809	+14:12:48.6828	0.45386705	7062.2837847	0.673±0.023	1.251±0.043	0.391±0.050	Y	-
210467408	11.25	3:54:40.2386	+14:50:42.936	1.40405312	7062.8117709	32.003±0.243	4.443±0.026	1.903±0.025	-	-
210470747	13.01	4:11:14.7617	+14:54:20.8836	4.42929490	7065.0476017	39.527±0.266	5.211±0.021	2.338±0.024	Y	-
210475773	12.69	4:14:43.8691	+14:59:46.3848	2.73570268	7063.6301069	19.499±0.051	6.054±0.016	2.182±0.013	Y	-
210476794	13.26	4:14:22.3289	+15:00:51.372	2.59908524	7064.2763514	5.061±0.060	5.349±0.070	1.658±0.054	Y	-
210483889	13.52	3:54:03.5693	+15:08:13.7472	7.19555800	7061.8819791	3.409±0.258	3.638±0.241	1.399±0.217	-	Y
210484192	8.89	3:54:03.3689	+15:08:30.1956	7.19777680	7069.0685760	2.362±*	4.376±0.142	2.188±*	-	Y
210501149	13.26	3:53:22.6973	+15:25:55.2756	20.73037900	7078.2641749	12.601±0.126	17.043±0.136	6.614±0.120	Y	-
210512162	11.60	3:38:29.5162	+15:36:49.95	4.11029828	7064.4035074	9.205±0.116	4.730±0.048	1.962±0.045	Y	-
210522228	12.59	4:15:50.431	+15:46:43.1904	10.80666413	7063.9073834	12.251±0.085	6.259±0.048	1.680±0.038	-	-
210525500	12.60	3:35:48.8453	+15:49:52.1904	1.36857312	7061.9003745	5.856±0.090	5.593±0.043	2.542±0.055	Y	-
210530173	12.85	3:57:39.4596	+15:54:16.4556	18.82451954	7080.4826230	12.388±1.010	4.493±0.309	1.834±0.267	Y	Y
210568002	14.38	3:58:16.0934	+16:29:29.2848	1.52306625	7064.9962196	0.102±0.005	3.286±0.178	0.983±0.148	Y	Y
210568214	9.45	3:58:12.0348	+16:29:41.604	1.52241202	7062.9904716	17.035±0.328	4.387±0.109	1.726±0.095	Y	-
210574135	12.46	3:45:20.6789	+16:35:03.408	0.92945698	7062.7854441	51.501±0.426	3.817±0.022	1.692±0.023	Y	-
210581202	10.44	4:01:07.9152	+16:41:19.032	5.55638852	7066.0027141	7.157±0.095	5.851±0.091	1.732±0.068	Y	-
210654881	12.63	3:55:50.4706	+17:44:11.6916	12.15749800	7064.0237504	12.841±0.152	5.335±0.052	2.186±0.051	-	-
210664740	10.80	4:29:15.6257	+17:52:15.6468	0.82989236	7062.0296866	7.119±0.363	2.074±0.088	0.804±0.089	Y	Y
210675130	9.44	3:53:00.1195	+18:00:47.7576	0.68909436	7062.1868951	11.040±0.239	4.023±0.088	1.617±0.072	-	-
210720575	9.31	3:47:57.0374	+18:39:48.0636	0.28672623	7061.9607860	0.933±0.023	1.878±0.056	0.589±0.050	-	-
210734337	11.68	3:56:22.1297	+18:52:13.4112	9.37822129	7067.6893126	45.070±0.265	10.460±0.051	4.634±0.045	-	-
210742688	12.82	3:52:37.7621	+18:59:50.1252	11.40879533	7072.2086935	1.478±*	3.658±0.074	1.829±*	-	Y
210749423	10.81	3:41:41.3882	+19:06:00.1008	1.57591030	7062.0222329	20.508±0.187	7.240±0.058	2.961±0.049	-	-
210750052	11.40	3:41:25.5137	+19:06:34.7904	4.62133974	7062.0240854	2.169±0.034	3.781±0.040	1.570±0.041	-	-
210754756	12.40	4:12:12.4222	+19:10:57.666	0.73952548	7062.4687832	0.819±0.030	1.185±0.104	0.229±0.097	Y	Y
210779706	12.66	4:25:14.4624	+19:33:41.6376	31.54381032	7082.2436262	18.500±1.604	4.982±0.495	1.725±0.390	Y	Y
210784039	12.52	3:44:52.2233	+19:37:37.3044	3.51383196	7065.3494459	5.291±0.045	4.614±0.033	1.812±0.028	Y	-
210786627	12.67	3:26:22.1729	+19:39:56.3544	1.71774108	7061.8945863	0.150±0.010	4.749±0.173	2.055±0.198	Y	Y
210786891	11.02	3:26:23.8956	+19:40:10.2118	1.71786749	7061.8914012	37.584±0.243	5.358±0.034	2.125±0.028	Y	-
210789323	13.50	3:41:48.8705	+19:42:21.9024	29.14159392	7073.7074664	7.678±0.149	2.580±0.048	1.287±0.024	-	-
210793743	13.96	3:42:21.2194	+19:46:28.5924	2.27187530	7064.0903218	21.947±0.682	2.080±0.032	0.928±0.045	Y	Y

Table 5. continued.

EPIC	mag	RA	DEC	Period	T0	Depth %	T_{14} (h)	T_{12} (h)	Sec	Gr
210805120	12.52	4:08:12.9991	+19:56:39.2892	3.00765150	7063.0531765	20.741±0.446	8.022±0.216	2.077±0.155	Y	-
210822691	11.89	3:41:14.2608	+20:12:53.5464	8.07555313	7064.1571139	27.552±0.575	5.363±0.108	2.181±0.088	Y	-
210837460	12.42	3:35:42.4087	+20:26:25.674	5.40395525	7063.8559645	2.049±0.024	3.008±0.033	1.117±0.030	Y	-
210846736	11.82	4:08:30.7666	+20:34:46.4952	5.19990746	7064.4957478	39.403±0.532	4.290±0.041	1.901±0.041	Y	-
210865148	12.63	3:57:28.0714	+20:51:23.94	3.24199797	7064.8190458	11.397±0.280	7.314±0.127	3.183±0.121	-	-
210876158	11.84	3:47:21.2767	+21:01:17.2992	0.92628502	7062.6442900	11.818±0.329	2.925±0.090	1.462±0.045	Y	-
210935498	11.28	3:53:19.957	+21:57:06.4692	1.18303091	7063.0264219	1.545±0.023	2.051±0.039	0.659±0.034	Y	-
210945342	12.01	3:51:13.1136	+22:06:37.8612	7.16463785	7063.1555873	2.215±0.177	10.578±0.491	4.917±0.537	Y	Y
210954046	12.44	4:03:36.9038	+22:14:56.9652	0.95030666	7062.7566171	0.467±0.025	2.365±0.126	0.863±0.115	Y	Y
210958990	12.61	4:11:00.9636	+22:19:31.2276	1.70233252	7062.3772436	2.269±0.026	2.609±0.048	0.562±0.041	Y	-
210960936	11.70	3:32:03.2767	+22:21:24.2892	1.43134555	7062.2426475	18.954±0.155	3.744±0.031	1.406±0.026	Y	-
210961508	13.56	3:59:40.825	+22:21:57.5424	0.35003422	7062.1003005	0.043±0.002	0.864±0.089	0.027±0.078	-	Y
210969614	11.21	4:05:10.1335	+22:29:48.1092	2.75751720	7063.5398997	41.749±0.473	7.842±0.085	3.171±0.068	Y	-
211000135	12.13	3:42:22.5084	+22:58:34.8528	1.81780108	7062.4283824	6.346±0.290	4.506±0.104	2.038±0.133	Y	Y
211002562	12.48	3:28:51.3648	+23:00:55.9584	3.34801857	7062.1025577	1.185±0.013	3.553±0.058	0.738±0.047	Y	-
211015722	12.02	4:02:00.5544	+23:13:26.8608	2.18398055	7063.2892814	15.554±0.055	3.182±0.013	1.056±0.011	Y	-
211020446	12.65	3:32:55.1395	+23:17:46.032	0.86204234	7062.4444313	25.522±0.243	3.642±0.035	1.391±0.029	Y	-
211041532	11.43	3:40:12.4339	+23:38:03.156	17.36785898	7075.4135402	4.246±0.234	6.475±0.323	2.854±0.269	-	Y
211093684	11.88	3:49:42.2762	+24:27:46.8144	7.05421275	7064.7030583	5.769±0.174	2.540±0.084	1.270±0.042	Y	-
211099781	12.10	3:44:12.9646	+24:33:26.6148	7.56151299	7064.4799641	1.626±0.036	6.733±0.180	1.295±0.138	Y	-
211147178	11.58	3:51:46.7534	+25:22:55.3692	5.73382176	7063.8446170	9.370±0.152	7.196±0.133	2.257±0.099	Y	-
211155479	8.91	3:53:07.4179	+25:32:07.2708	13.05503202	7064.2962369	22.857±1.234	6.505±0.255	2.815±0.255	-	Y
211160700	9.31	3:51:21.5527	+25:38:07.3896	0.63154087	7061.9827166	14.486±0.152	3.579±0.029	1.512±0.028	-	-
211160717	9.44	3:51:21.2213	+25:38:08.3724	0.63157505	7061.9810507	14.518±0.143	3.622±0.027	1.528±0.027	-	-
Campaign 5										
211309989	13.94	8:28:45.1642	+10:03:06.642	7.53920187	7145.6594007	29.617±0.498	3.286±0.054	1.391±0.042	-	-
211324599	14.21	8:55:04.794	+10:20:39.948	8.77142724	7147.4354275	10.984±0.472	2.035±0.072	0.839±0.072	-	Y
211345799	9.68	8:27:11.953	+10:44:13.4664	2.87622736	7144.0949063	6.749±0.073	5.450±0.053	2.142±0.046	Y	-
211371463	12.93	8:50:27.1337	+11:10:57.0396	5.66728183	7147.3845871	11.286±0.144	6.948±0.094	2.301±0.073	Y	-
211396167	14.49	8:47:06.6072	+11:34:58.044	4.44865106	7141.3157897	23.438±0.784	3.095±0.062	1.360±0.075	Y	Y
211408138	12.74	8:51:17.9916	+11:45:54.198	10.33768855	7149.7181944	4.847±0.091	7.204±0.196	1.637±0.132	Y	-
211409299	11.95	8:43:42.1202	+11:46:57.4248	13.92102594	7149.6448437	11.879±0.128	4.998±0.035	2.086±0.035	-	-
211409713	12.49	8:29:22.0051	+11:47:19.4352	3.09978700	7144.1932186	11.371±0.036	3.755±0.014	1.156±0.011	Y	-
211416577	11.21	8:51:20.8102	+11:53:26.034	1.06773697	7142.8635346	5.114±0.155	3.626±0.091	1.362±0.083	Y	-
211421547	12.86	8:26:22.4352	+11:57:49.0932	3.15061630	7144.8687101	14.643±0.085	4.943±0.027	1.956±0.023	Y	-
211432167	8.55	8:51:27.3134	+12:07:40.5084	5.81781612	7147.7467833	1.026±0.013	3.655±0.058	0.974±0.046	Y	-
211432946	14.40	8:50:32.951	+12:08:23.3988	3.34388559	7141.3737551	37.367±1.180	1.942±0.055	0.791±0.056	Y	Y
211462458	11.19	9:05:37.0481	+12:35:23.0784	3.60195759	7144.9851960	10.841±0.049	4.401±0.017	1.735±0.015	Y	-
211490999	13.42	8:43:11.7233	+13:00:34.5348	19.68543884	7146.3296410	0.100±0.004	3.091±0.000	0.002±0.000	Y	-
211518347	12.58	8:21:31.2535	+13:23:51.3672	1.87120628	7142.7565987	25.875±0.159	2.887±0.017	1.152±0.015	Y	-
211526186	12.81	9:01:05.8361	+13:30:33.2568	0.45510182	7142.4039723	1.971±*	1.961±0.027	0.980±*	Y	Y
211563123	12.58	8:44:30.9696	+14:01:35.3748	17.32052062	7145.3989468	33.793±0.880	8.031±0.180	3.340±0.156	-	-
211567126	10.03	8:14:01.681	+14:05:01.5612	7.43065859	7142.2604708	5.778±0.219	8.622±0.240	3.532±0.220	Y	-
211569350	12.11	8:13:00.6526	+14:06:54.7272	1.65573752	7142.3592623	4.306±0.119	3.970±0.063	1.758±0.074	Y	Y

Table 5. continued.

EPIC	mag	RA	DEC	Period	T0	Depth %	T_{14} (h)	T_{12} (h)	Sec	Gr
211573482	13.25	8:17:09.3509	+14:10:15.366	7.06903244	7143.6562262	14.728±0.588	3.369±0.162	1.037±0.123	Y	-
211578677	14.29	9:07:10.681	+14:14:39.6492	0.27712271	7142.2487482	6.157±0.325	1.732±0.017	0.818±0.054	-	Y
211581700	12.16	8:37:57.3252	+14:17:17.7972	1.29107605	7142.1224776	28.537±0.186	4.224±0.023	1.739±0.021	Y	-
211604396	13.21	8:37:37.2324	+14:35:55.0752	0.87270897	7142.1404749	55.923±1.517	3.862±0.053	1.769±0.069	Y	Y
211611158	12.41	8:41:02.3179	+14:41:25.152	52.79086836	7159.1242039	0.072±0.011	7.185±0.565	3.311±0.701	-	Y
211613886	12.73	9:02:47.9107	+14:43:40.7136	0.95880876	7142.1168840	2.557±0.381	1.653±0.022	0.805±0.132	Y	Y
211631904	13.99	8:40:42.0871	+14:59:02.1552	0.44199762	7142.2588391	29.038±1.537	1.239±0.054	0.417±0.066	Y	Y
211682657	8.98	8:54:33.0266	+15:40:55.0164	3.14072418	7145.1786054	5.183±0.057	6.251±0.078	1.372±0.059	Y	-
211685048	14.27	8:13:27.0317	+15:42:49.6008	0.76913557	7142.1610653	16.738±0.341	2.095±0.036	0.722±0.039	Y	-
211693443	9.05	8:15:09.4392	+15:49:39.4932	2.17291914	7143.9654167	2.718±0.091	4.996±0.158	1.879±0.132	Y	-
211693443	9.05	8:15:09.4392	+15:49:39.4932	2.17291914	7143.9654167	2.718±0.091	4.996±0.158	1.879±0.132	Y	-
211719362	10.48	8:41:38.227	+16:10:34.6404	0.20110164	7142.0833134	0.912±6655.813	1.364±0.014	0.682±4979.310	-	Y
211726283	11.18	8:18:06.0451	+16:16:19.02	2.78612336	7144.3670919	14.717±0.194	4.890±0.067	1.721±0.056	Y	-
211726889	14.50	8:36:43.3903	+16:18:25.0164	8.95271527	7146.5631761	9.855±0.026	4.142±0.009	1.625±0.008	-	-
211730838	12.65	8:15:37.7525	+16:20:14.2296	1.30707667	7143.0087613	6.307±0.173	3.763±0.112	1.238±0.090	Y	-
211732801	10.65	8:37:52.7105	+16:21:56.6604	4.26259856	7143.5400949	7.378±0.049	4.574±0.027	1.826±0.024	Y	-
211770390	12.24	8:45:24.8407	+16:53:44.7828	7.57747238	7148.1729595	7.812±0.148	7.501±0.134	3.007±0.106	Y	-
211785852	9.95	8:23:58.3229	+17:06:50.7096	7.15609805	7147.3475251	29.861±0.304	6.521±0.059	2.703±0.050	Y	-
211797674	10.55	8:29:39.3163	+17:17:00.6108	1.32311792	7142.3965441	41.033±0.430	3.197±0.025	1.358±0.025	Y	-
211805860	13.77	8:19:52.0294	+17:23:59.7516	4.14248936	7142.7183408	25.275±0.372	3.112±0.032	1.314±0.034	Y	-
211807843	11.44	8:36:07.0418	+17:25:37.9884	6.76399673	7145.9926120	43.835±0.532	5.791±0.030	2.705±0.043	Y	-
211812160	13.48	8:52:15.5146	+17:29:20.4972	2.17024600	7141.0309342	1.525±0.016	2.280±0.014	0.973±0.018	Y	-
211817572	11.39	8:12:23.053	+17:33:54.5544	2.25912762	7142.2819243	0.551±0.366	1.547±0.105	0.745±0.564	Y	Y
211820126	12.18	8:15:23.6448	+17:36:07.2144	4.75751564	7145.7663387	14.128±0.187	6.843±0.057	3.013±0.060	Y	-
211825356	12.61	8:27:13.5029	+17:40:35.7888	3.26237418	7143.4904404	27.313±0.514	10.394±0.116	4.664±0.122	Y	-
211834405	13.58	8:49:29.777	+17:48:15.1704	10.53981404	7142.4363636	42.610±0.496	5.121±0.048	2.183±0.043	Y	-
211839430	10.73	8:50:02.0131	+17:52:27.1416	5.22253791	7143.6375744	14.805±0.166	9.859±0.128	2.821±0.096	Y	-
211839462	10.04	8:50:01.421	+17:52:28.434	5.22535041	7143.6176786	15.597±0.083	9.706±0.062	2.817±0.048	Y	-
211885185	12.49	8:44:06.5837	+18:30:39.7764	8.79767294	7150.4780144	29.847±0.386	6.507±0.084	2.458±0.067	Y	-
211902535	10.88	8:28:55.6781	+18:45:49.5216	9.81087400	7142.8476121	15.774±0.265	7.926±0.126	3.143±0.100	Y	-
211915147	9.02	8:39:09.3	+18:57:06.7284	1.81126620	7142.1868694	3.663±0.173	3.628±0.112	1.536±0.119	-	Y
211936444	12.92	8:25:59.8934	+19:16:17.58	4.92911006	7143.5705161	6.767±0.020	3.579±0.009	1.425±0.008	Y	-
211942157	12.05	8:50:51.1918	+19:21:26.1756	1.32456289	7142.8399936	23.617±0.543	5.368±0.114	2.049±0.096	Y	-
211944670	10.55	8:31:37.565	+19:23:39.4152	2.77155959	7142.7194802	12.435±*	1.683±0.031	0.841±*	Y	Y
211944676	9.90	8:31:37.5974	+19:23:39.5556	2.77155959	7142.7194509	12.312±5.726	1.680±0.033	0.831±0.398	Y	Y
211958340	10.05	8:32:02.31	+19:36:02.0952	1.46548150	7143.1092252	7.950±0.065	2.883±0.037	0.704±0.030	Y	-
211972837	13.55	8:39:54.6221	+19:49:18.912	1.09304414	7142.3142123	89.142±0.246	3.922±0.016	1.961±0.008	Y	-
211978865	14.44	8:15:35.4761	+19:54:53.4996	0.90781917	7142.3795006	1.781±0.146	2.068±0.067	0.879±0.108	Y	Y
211979325	13.18	8:35:47.6426	+19:55:18.2964	2.07763117	7143.0766499	2.272±0.151	4.983±0.322	1.766±0.272	Y	Y
211982753	8.78	8:19:00.0773	+19:58:33.5964	5.38963128	7147.1215187	22.574±0.245	5.413±0.040	2.361±0.040	Y	-
211995966	11.90	8:44:50.124	+20:11:16.4868	0.27924738	7142.1669398	13.679±2.095	1.481±0.011	0.729±0.119	-	Y
211996855	10.43	8:44:27.9542	+20:12:07.452	1.20630980	7142.0794831	5.215±*	1.972±0.053	0.985±*	Y	Y
211997641	12.82	9:07:36.6077	+20:12:54.4356	1.74482162	7142.2473934	28.257±0.170	5.036±0.021	2.208±0.021	Y	-
211999656	12.23	8:25:58.5502	+20:14:55.6476	0.97413338	7142.4752041	12.753±0.056	2.998±0.012	1.206±0.011	-	-

Table 5. continued.

EPIC	mag	RA	DEC	Period	T0	Depth %	T_{14} (h)	T_{12} (h)	Sec	Gr
212009702	13.17	9:04:52.7153	+20:24:54.4536	0.92389717	7142.9435212	39.248±0.793	3.248±0.029	1.488±0.042	Y	-
212012387	13.97	8:53:06.9542	+20:27:32.1876	6.48723194	7143.5299904	54.403±780.065	3.318±0.043	1.659±*	Y	Y
212019055	12.70	8:29:07.8977	+20:34:12.8172	0.82143486	7142.4592194	19.062±0.288	2.410±0.027	1.004±0.029	Y	-
212020442	13.97	9:10:02.9935	+20:35:37.8744	7.77791809	7143.8202717	6.752±0.157	3.329±0.051	0.902±0.046	Y	-
212024647	10.28	8:31:44.4578	+20:39:49.6152	3.69692653	7142.0963880	14.648±0.233	3.235±0.046	1.249±0.042	Y	-
212029934	12.04	8:36:22.8766	+20:45:09.9972	0.62474746	7142.4869560	2.412±0.207	1.682±0.112	0.655±0.129	-	Y
212037403	13.23	8:32:42.8794	+20:52:40.152	3.40813253	7144.1442214	20.152±0.275	2.867±0.036	1.140±0.032	Y	-
212082682	14.61	8:53:09.2364	+21:41:25.6524	3.79703875	7142.6518727	11.336±0.194	2.550±0.039	0.959±0.037	Y	-
212083250	11.97	8:51:04.7801	+21:42:04.8672	0.51873578	7142.4701837	23.038±0.462	2.464±0.031	1.048±0.037	Y	-
212085740	13.69	8:30:25.0258	+21:44:49.3944	4.84614565	7146.4283292	8.851±0.276	3.133±0.081	1.267±0.076	Y	-
212096658	10.21	8:27:00.8974	+21:57:24.6996	2.93291207	7143.4724988	19.614±0.415	2.421±0.035	0.996±0.038	Y	-
212116340	12.08	8:53:41.0182	+22:20:39.0876	0.61022558	7142.0785008	18.410±0.774	2.816±0.084	1.169±0.089	Y	Y
212122623	13.93	8:37:02.3066	+22:28:01.4988	1.31337513	7142.5434036	5.873±0.146	1.860±0.080	0.477±0.069	Y	-
212152922	11.82	8:30:35.755	+23:05:49.9272	4.87928873	7144.1830711	0.816±0.028	2.162±0.078	0.772±0.075	Y	-
212155299	13.13	8:26:27.228	+23:08:58.8156	0.90161059	7142.4192680	30.022±0.336	2.378±0.030	0.868±0.026	Y	-
212163353	13.54	8:56:51.1133	+23:19:49.674	10.34540230	7146.9323699	8.618±0.133	3.806±0.044	1.550±0.043	Y	-
Campaign 6										
212270970	13.35	13:51:09.9576	-18:27:42.2172	0.71650978	7225.3082153	0.225±0.505	1.799±0.114	0.897±2.035	Y	Y
212280240	12.90	13:37:29.0616	-18:08:33.3636	0.77048715	7225.7513224	0.889±0.074	1.130±0.108	0.250±0.118	Y	Y
212290847	12.32	13:31:07.2182	-17:48:40.77	8.39646054	7230.6873950	16.282±0.089	6.069±0.030	2.474±0.025	Y	-
212302722	12.55	13:21:50.6705	-17:26:57.966	0.78374363	7225.1793906	22.124±0.419	3.397±0.029	1.552±0.042	Y	-
212304395	14.29	13:37:13.2638	-17:23:50.4888	1.60602808	7226.0913413	0.538±0.036	2.098±0.131	1.049±0.065	Y	-
212310740	10.59	13:35:04.566	-17:12:40.3884	3.59977695	7225.7812400	6.923±0.086	2.587±0.035	0.931±0.030	Y	-
212323325	14.69	13:27:42.8306	-16:51:16.5492	0.66423973	7225.5385515	1.958±0.114	2.110±0.107	0.816±0.108	Y	Y
212327309	14.53	13:34:58.5564	-16:44:27.1536	6.71643269	7230.9026795	34.955±0.269	3.545±0.021	1.507±0.021	-	-
212334671	14.55	13:53:01.6942	-16:32:24.6048	15.45384129	7230.3075857	6.571±0.251	5.816±0.187	2.187±0.163	-	-
212339438	12.96	13:31:53.3098	-16:24:40.788	2.70427077	7227.6687629	7.070±0.029	4.239±0.018	1.382±0.014	Y	-
212349750	12.77	13:32:18.7272	-16:08:16.62	2.86836478	7226.9463131	27.541±0.232	5.237±0.044	1.911±0.035	Y	-
212351048	10.04	13:26:40.5792	-16:06:16.4988	2.54942826	7225.8004623	69.706±0.755	7.877±0.096	3.497±0.071	Y	-
212351868	10.22	13:39:59.2874	-16:04:58.3644	2.50044839	7225.5581540	6.377±0.057	5.137±0.056	1.086±0.044	Y	-
212362957	13.94	13:23:07.1587	-15:47:58.0416	12.51587639	7230.4214104	14.221±0.092	4.645±0.025	1.907±0.022	-	-
212370052	12.99	13:26:08.3424	-15:37:35.7528	7.77625604	7230.8612243	35.717±0.245	6.053±0.039	2.472±0.032	Y	-
212383778	13.33	13:37:58.3217	-15:17:25.962	1.65376760	7225.6613225	33.356±0.528	7.517±0.114	2.976±0.092	Y	-
212384646	13.40	14:02:43.8478	-15:16:08.8356	1.73492254	7226.3146815	18.797±0.334	6.796±0.085	2.948±0.083	Y	-
212406350	13.92	13:33:57.349	-14:46:07.4532	0.83375327	7225.1435877	6.753±0.302	1.245±0.255	0.104±0.237	Y	Y
212409377	13.04	13:28:11.4007	-14:42:02.0808	2.23115139	7225.1349177	52.752±*	2.795±0.009	1.397±*	Y	Y
212409856	13.45	13:36:54.792	-14:41:23.9856	0.53159032	7225.4460002	25.250±0.529	2.546±0.029	1.119±0.037	Y	-
212426112	13.15	13:40:20.1583	-14:19:30.6264	1.53026278	7225.0332668	4.036±*	1.877±0.041	0.939±*	Y	Y
212428509	12.48	13:34:30.8393	-14:16:17.8356	5.33484570	7225.1739457	1.145±0.031	2.719±0.046	1.119±0.052	Y	-
212453473	13.96	13:17:46.6632	-13:43:39.3312	5.51241950	7222.8415521	41.724±0.361	3.414±0.019	1.514±0.021	Y	-
212456583	13.43	13:27:47.3894	-13:39:33.102	5.7568777	7229.7328799	26.086±0.459	4.003±0.059	1.601±0.052	Y	-
212469831	13.56	13:28:16.5034	-13:22:46.5204	5.07526108	7228.4483215	0.652±0.010	2.330±0.024	0.991±0.028	-	-
212473154	8.98	13:27:40.811	-13:18:37.044	3.63462964	7225.4394757	0.362±0.016	3.172±0.104	1.170±0.103	Y	-
212481328	13.09	13:13:53.3918	-13:08:15.3168	3.41698906	7226.1532424	4.245±0.029	2.646±0.017	1.025±0.015	Y	-

Table 5. continued.

EPIC	mag	RA	DEC	Period	T0	Depth %	T_{14} (h)	T_{12} (h)	Sec	Gr
212488008	10.63	13:10:56.2289	-12:59:33.0468	11.33254465	7226.0966911	0.187±0.035	2.323±0.100	1.065±0.260	Y	Y
212497267	12.28	13:27:43.3346	-12:47:32.3196	3.74549396	7226.9989212	29.606±0.262	4.083±0.040	1.595±0.032	Y	-
212504385	13.84	13:18:17.1641	-12:38:26.3616	0.82685020	7225.6890032	16.476±0.340	2.889±0.044	1.203±0.047	Y	-
212512986	12.80	13:42:43.4825	-12:27:25.9308	1.50012308	7226.2914488	61.274±0.898	5.700±0.062	2.573±0.059	Y	-
212535959	13.80	13:51:40.3598	-11:58:08.9184	17.70615157	7232.8017839	11.704±0.586	7.273±0.297	2.543±0.236	-	-
212536771	13.74	13:49:50.5855	-11:57:07.8804	2.78373389	7226.1559193	20.292±0.266	3.581±0.040	1.433±0.037	Y	-
212537106	12.98	13:40:48.5846	-11:56:43.4422	9.26332824	7227.3709879	17.724±0.234	6.569±0.093	2.339±0.072	Y	-
212541386	14.23	13:35:28.339	-11:51:33.6744	3.63147365	7226.9518172	7.972±0.201	2.396±0.064	0.874±0.059	Y	-
212559866	11.86	13:32:10.9452	-11:27:46.1772	19.70331061	7238.3041802	12.056±0.041	8.763±0.029	3.522±0.024	-	-
212560752	12.84	13:36:11.2361	-11:26:34.5588	0.58278074	7225.2956615	16.229±0.341	3.974±0.071	1.562±0.064	-	-
212576383	9.07	13:11:17.4096	-11:06:21.2436	5.98450008	7228.4150855	20.663±0.143	7.346±0.043	2.960±0.037	Y	-
212579164	13.63	13:12:17.945	-11:02:51.558	18.15627406	7238.5528315	19.780±0.479	3.009±0.067	1.192±0.058	Y	-
212586717	13.88	13:55:16.0162	-10:52:58.9944	8.59369149	7223.7543438	2.183±0.075	2.504±0.066	0.994±0.067	Y	-
212610849	14.45	13:37:37.931	-10:20:39.588	28.49556559	7246.3229326	1.844±0.220	2.824±0.443	1.412±0.221	-	-
212613128	13.86	13:30:11.1845	-10:17:34.4688	0.75917361	7225.1061484	26.640±0.830	1.750±0.026	0.758±0.040	Y	Y
212615080	13.64	14:00:01.2862	-10:14:54.9456	7.37649383	7230.7662109	18.548±0.234	3.271±0.039	1.148±0.036	-	-
212617879	12.32	13:37:37.643	-10:11:02.0256	4.42082948	7226.9934128	22.369±0.351	4.102±0.062	1.596±0.053	Y	-
212627712	13.27	13:17:43.7453	-9:57:30.6576	19.90196677	7230.3998930	7.001±0.360	3.797±0.225	1.898±0.113	-	-
212628098	13.26	13:21:09.7337	-9:56:57.0048	4.35251469	7227.6988379	5.361±0.090	1.673±0.036	0.606±0.033	-	-
212633681	14.35	13:30:04.1796	-9:49:19.668	8.83696551	7223.3791584	43.538±1.457	4.864±0.083	2.212±0.103	Y	Y
212645173	13.56	13:42:20.1154	-9:33:22.4424	6.97894931	7229.4293758	36.422±0.275	3.504±0.020	1.487±0.020	Y	-
212651213	10.80	13:55:43.465	-9:25:05.916	5.07645525	7228.4955088	5.787±0.144	4.283±0.073	1.825±0.074	Y	-
212651234	11.14	13:55:42.7632	-9:25:04.0188	5.07699928	7228.4909132	5.555±0.102	4.248±0.061	1.711±0.057	Y	-
212658818	12.07	13:12:58.2842	-9:14:27.2976	4.64082736	7226.7269029	1.101±0.058	3.166±0.039	1.493±0.097	Y	Y
212664590	13.59	13:44:43.296	-9:06:22.2948	14.70165031	7239.2472848	54.113±1.300	4.185±0.061	1.853±0.070	-	-
212666524	14.29	13:44:26.059	-9:03:40.7808	0.67053269	7225.0496422	18.746±0.344	3.126±0.039	1.334±0.042	Y	-
212678026	13.33	14:01:08.603	-8:47:22.2216	10.37459740	7235.6172915	15.557±556.763	8.705±0.396	4.353±*	Y	Y
212679925	13.02	13:29:56.2958	-8:44:47.9976	1.83505407	7226.0533737	2.973±*	2.175±0.046	1.087±*	-	Y
212687040	13.48	13:28:36.5486	-8:34:39.3852	1.85288313	7225.9788064	26.778±0.385	2.507±0.035	0.951±0.033	Y	-
212691727	12.66	13:20:28.6565	-8:27:52.2936	12.87212873	7232.3648881	6.135±0.194	5.336±0.193	1.717±0.142	Y	-
212697951	12.58	13:52:07.9176	-8:18:42.462	1.91254442	7225.9979206	16.540±0.170	2.626±0.022	1.069±0.022	Y	-
212701118	12.69	13:41:08.3921	-8:13:54.3936	2.43390471	7225.6062099	54.519±0.592	3.108±0.024	1.379±0.025	Y	-
212702889	14.56	13:33:39.8719	-8:11:09.8484	0.63103583	7225.1021964	5.394±0.148	1.507±0.017	0.660±0.030	Y	Y
212707624	13.18	13:18:53.3839	-8:04:17.1984	7.21270739	7226.5532027	19.014±0.322	5.119±0.059	2.240±0.059	Y	-
212708783	10.39	13:56:54.1925	-8:02:31.1676	2.25395336	7226.5964513	13.543±0.195	3.821±0.057	1.456±0.048	Y	-
212727054	8.68	13:25:21.0389	-7:35:02.8752	15.50013241	7237.5690541	10.973±0.634	6.587±0.218	3.011±0.239	-	Y
212727070	9.44	13:25:21.431	-7:35:01.5972	15.51028181	7237.5558127	7.750±0.571	5.961±0.419	2.506±0.329	-	Y
212751916	13.89	13:28:56.743	-6:55:38.9532	15.71138853	7237.6378984	0.887±0.031	3.971±0.109	1.662±0.107	-	Y
212757004	12.10	13:44:31.5242	-6:47:06.4716	4.45819015	7226.3297294	3.024±*	3.526±0.058	1.763±*	Y	Y
212757039	14.38	13:44:31.8262	-6:47:03.4044	4.45776115	7226.3329538	2.507±0.046	3.238±0.068	1.115±0.056	Y	-
212773309	11.39	13:49:32.3808	-6:19:21.8676	4.68201630	7227.3456141	6.489±0.306	2.208±0.084	0.891±0.089	-	Y
212775692	11.42	13:34:49.854	-6:15:06.7284	0.64123204	7225.3210810	8.287±0.109	2.968±0.041	1.484±0.020	Y	-
212786474	14.47	13:35:18.1838	-5:56:19.968	9.27132671	7233.9059728	36.737±1.048	3.378±0.067	1.475±0.071	Y	Y
212788116	13.82	13:37:46.8655	-5:53:33.4068	9.24586700	7234.1018505	11.311±0.495	3.506±0.144	1.268±0.119	Y	-

Table 5. continued.

EPIC	mag	RA	DEC	Period	T0	Depth %	T_{14} (h)	T_{12} (h)	Sec	Gr
212805198	14.42	13:27:44.8488	-5:22:59.5488	3.22765043	7225.2440645	5.166±0.330	2.289±0.097	0.913±0.127	Y	Y
212805296	14.22	13:27:45.6713	-5:22:48.828	3.22765043	7225.2444089	5.003±0.514	2.322±0.103	1.005±0.169	Y	Y
212812349	13.71	13:31:13.8641	-5:09:17.568	8.16625799	7230.0341464	7.938±0.059	4.521±0.033	1.543±0.027	Y	-
212822491	11.08	13:44:19.4376	-4:49:38.964	14.30219618	7226.6155083	16.712±1.447	6.452±0.458	2.323±0.420	Y	Y
212841253	10.50	13:27:10.2463	-4:10:20.5788	0.75426586	7225.1975453	21.850±0.418	3.573±0.073	1.228±0.060	Y	-